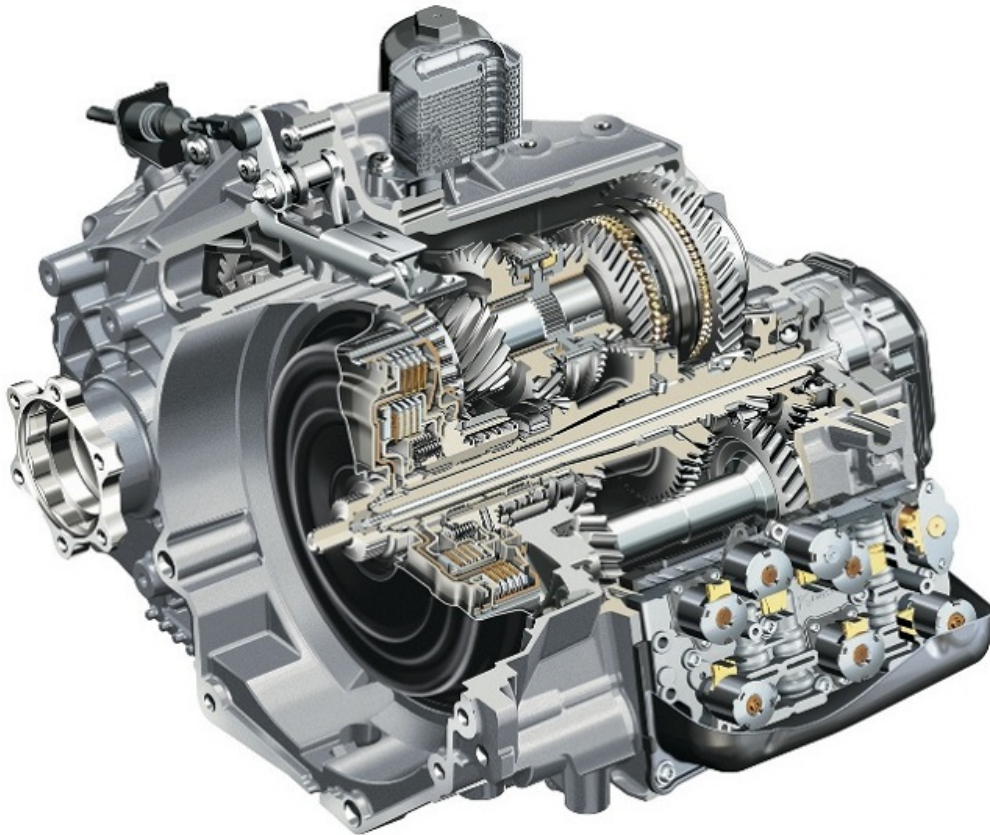




CHALMERS
UNIVERSITY OF TECHNOLOGY



NVH Validation of a Dual Clutch Transmission for Clonk

Structural Vibration & Acoustical Radiation Evaluation

Master's Thesis in Sound & Vibrations
Emrah Yilmaz, Shaohai Xiong

Department of Architecture and Civil Engineering
Division of Applied Acoustics
CHALMERS UNIVERSITY OF TECHNOLOGY
Gothenburg, Sweden 2018

MASTER'S THESIS ASEX30-18-97

NVH Validation of a Dual Clutch Transmission for Clonk

Emrah Yilmaz, Shaohai Xiong



Department of Architecture and Civil Engineering
Division of Applied Acoustics
CHALMERS UNIVERSITY OF TECHNOLOGY
Gothenburg, Sweden 2018

NVH Validation of a Dual Clutch Transmission for Clonk
EMRAH YILMAZ
SHAOHAI XIONG

© EMRAH YILMAZ, 2018.

© SHAOHAI XIONG, 2018.

Supervisor: Rajesh Kumar Moolam, CEVT

Supervisor: Pontus Paulsson, CEVT

Examiner: Wolfgang Kropp, Applied Acoustics, CHALMERS

Master's Thesis ACEX30-18-97

Department of Architecture and Civil Engineering

Division of Applied Acoustics

Chalmers University of Technology

SE-412 96 Gothenburg

Telephone +46 31 772 1000

Cover: 6 speed DCT, 6DCT450, GETRAG[1], not the one used in this thesis.

Typeset in L^AT_EX

Chalmers Reproservice/Department of Applied Acoustics

Gothenburg, Sweden 2018

NVH Validation of a Dual Clutch Transmission for Clonk

Shaohai Xiong, Emrah Yilmaz

Division of Applied Acoustics

Chalmers University of Technology

Abstract

A transmission housing is built like a big "bell" that is made to keep shafts and gears in place and keep them lubricated under operating loads. Being a big aluminum chunk with thin walls could attain some interesting sound and vibration properties. To reduce tonal noise and vibrations generated under operating loads is high priority for today's automotive manufacturers. The cars that use combustion engine usually mask most of the transmission noise, and the driver is not particularly affected. However, the electric engines are very silent which results in the driver mostly hearing different transmission noises like gear whine, rattling, clonk, shifting noise and bearing noise.

This thesis is aimed to investigate sound and vibration properties of clonk in a dual clutch transmission. To simplify the complex clonk phenomena that happens in an actual DCT, a simplified impulse force is used as an input force to evaluate vibration and sound properties. Using five different simulation methods with four different software, the DCT finite element model is analyzed to calculate sound and vibrations generated from the impulse load. The objective of simulation is to get a good understanding of the transmission NVH behaviour under transient loads within operating frequency range so that countermeasures can be applied to reduce or dampen the resonance peaks.

Measurements in the form of impact measurements have been performed in the anechoic chamber at the Applied Acoustics division of Chalmers University of Technology. The test setup contains impact measurement equipment with two accelerometers and two microphones. The measurement data acquired from the equipment has been used to validate and correlate with the simulation results, so that simulation methods are validated for sound and vibration properties.

In conclusion, the simulation results differ in the high frequency range while keeping close correlation in the lower frequencies (around 1 kHz), this can be the consequence of the hammer impact force and location of excitation in the measurement is not possible to excite all high frequencies, thus, the data used to compare at the high frequency range are insufficient. For future work, the validated FE models can be used for locating the most radiated surfaces on the transmission under operating loads, and the transmission housing can be improved by making the radiated surface stiffer or make use of damping layers.

Keywords: structural vibration, acoustic radiation, simulation, impact measurement, Dual Clutch Transmission, clonk, NVH, CAE

Acknowledgements

We would like to thank our supervisors from CEVT, Rajesh Kumar Moolam, Pontus Paulsson and Alejandro Martinez for their great help and guidance throughout this thesis. We would also like to give many thanks to our examiner Wolfgang Kropp for his guidance, input and mentoring. Many thanks to Jens Ahrens, Börje Wijk and all teaches and classmates in our department for their advice and support. We wish to express our thanks to our friendship and cooperation that through out the thesis working gave us the confidence to go on.

Also a big thanks to Milton Eduardo Pena from BETA CAE AB for his support with ANSA guidance. Many thanks to Tomas Wiklund for his great devote for helping implementing measurements. And last but certainly not least we would like to thank Alejandro Martinez, Marcin Serafin, Jonas Skoglund and all the colleagues in transmission system and simulation group for their support and advice.

I want to thank my family, in particular my mother and grandmother, have been supportive throughout my entire education. Without their encouragement and cooking skills throughout my five years of university, it would have been an almost impossible journey. /Emrah Yilmaz

Shaohai Xiong, Emrah Yilmaz
Gothenburg, Sweden, Summer 2018

Contents

List of Figures	xi
List of Tables	xiii
1 Introduction	1
1.1 Background	2
1.2 Objective	2
1.3 Limitation	2
2 Dual Clutch Transmission (DCT)	3
2.1 Basic Principle	3
2.2 Control	4
2.3 CAE Model	5
2.4 Clonk Noise and Propagation	6
3 Theory	7
3.1 Wave Theory	7
3.2 Finite Element Method	8
3.2.1 Frequency Limitation	9
3.3 Infinite Element Method	10
3.4 Equivalent Radiated Power	12
4 Simulation Methods and Results	13
4.1 Dynamic Implicit	13
4.2 Free Response	17
4.3 Direct Method versus Modal Method	18
4.3.1 Forced Response, Direct Method	19
4.3.2 Forced Response, Modal Method	20
4.4 Infinite Element Analysis	24
4.4.1 Acoustic Model Pre-Processing	24
4.4.2 RADACT Interface	27
4.4.3 Acoustic Model Post-Process	28
4.5 ERP Method	28
5 Measurement	31
5.1 Equipment	31
5.2 Setup	31

5.3	Measurement Positions	32
5.4	Signal Processing	35
5.5	Results	40
6	Validation	45
6.1	Vibration	46
6.2	Acoustics	49
7	Conclusion	51
	Bibliography	53
A	Appendix - Simulation	I
B	Appendix - Measurement	IX
B.1	1/3rd Octave band validation	XII

List of Figures

2.1	Basic diagram of a 6-speed passenger car DCT VW DS [®] [4].	3
2.2	Control system layout of shifting modes	4
2.3	Complete model	5
2.4	Base model	5
2.5	Propagation path of airborne and structure borne noise [6]	6
3.1	Sketch of wave patterns	8
3.2	Geometry at interface between infinite and finite elements	10
3.3	Mesh around the object ($\Omega^e = \Omega_\gamma^{i,e} \cup \Omega_\gamma^{o,e}$).	11
4.1	Complete model used to create simulation	14
4.2	Boundary condition used in simulation	14
4.3	Groups of contact	15
4.4	Groups of constraints	15
4.5	Vertical Hit	16
4.6	Mode shapes at 2467Hz	18
4.7	Torsional Hit	19
4.8	Mode shapes at 4000Hz	20
4.9	Base Model	21
4.10	RBE2	21
4.11	RBE3	21
4.12	Load case "HITCase"	22
4.13	Load case "HITOutput"	22
4.14	"HITCase", Isometric and Left View, at 2500 Hz	23
4.15	"HITOutput", Isometric and Left View, at 2500 Hz	24
4.16	Strategy of IEM	24
4.17	Wrapped Surface	25
4.18	Infinite Domain	26
4.19	Finite Fluid	26
4.20	Total Acoustic Model	27
4.21	ERP Panel, shell meshed with CTRIA6 elements	28
4.22	ERP results with original properties	29
5.1	Setup of hammer test	32
5.2	Hammer Excitation Positions (HIT Case left side, HIT Output right side)	33
5.3	Accelerometers position 1	33

5.4	Accelerometers position 2	34
5.5	Accelerometers position 3	34
5.6	Accelerometers position 4	34
5.7	Example of Good Measurements	36
5.8	Example of Bad Measurements	36
5.9	4 Hits From POS1CASE	37
5.10	Full frequency and cut-off from 500Hz	40
5.11	Coherence and FRF estimates	41
5.12	Mobility of H1 (Ymob1) and H2 (Ymob2)	41
5.13	Amplitude and Phase	42
5.14	Real and Imaginary	42
5.15	"HITCASE" positions 1, 2 and 4	43
5.16	"HITOUTPUT" positions, 1, 2 and 3	44
6.1	Illustration of the half-power bandwidth method	45
6.2	Validation of ACCBlack for Case hit, POS1	47
6.3	ACCBlack, Case, POS2	48
6.4	ACCBlack, Case, POS4	48
6.5	Validation of ACCBlack for Output hit, POS1	48
6.6	ACCBlack, Output, POS2	49
6.7	ACCBlack, Output, POS3	49
6.8	Mic Green, Case	50
6.9	Mic Green, Output	50
6.10	Mic Pink, Case	50
6.11	Mic Pink, Output	50
A.1	Acoustic Fluid Mesh Pre-Processing	III
A.2	Acoustic Fluid Mesh Properties	III
A.3	Acoustic Infinite Domain Definition	IV
A.4	Projection Surface Definition	IV
A.5	Acoustic Field Points Definition	V
A.6	Structure Import	V
A.7	Analysis Parameters	VI
A.8	Post-Processing Output Files Definition	VI

List of Tables

2.1	Name of the DCT main sections with power flow	4
2.2	Model used for the methods	5
2.3	Material properties of the casing	5
3.1	Comparison between FEM and IEM	10
3.2	Element properties in acoustics	11
4.1	Step parameters	16
4.2	Modal vs Direct method	19
4.3	DAREA	22
4.4	RLOAD	22
4.5	Frequency Range	23
4.6	ERP calculation type and frequency range	29
5.1	Equipment used in the measurements	31
6.1	Damping factors	46
6.2	Normal direction relative to the simulation	47

1

Introduction

The development of new vehicles is influenced by the demand of a more intense customer comfort claim regarding Noise, Vibration and Harshness (NVH) characteristics. The recent customer trend for a new vehicle have shown that a major factor in purchasing a car is the fun of driving it. This can be achieved with an increase of engine torque to realize a good agility. This results in a situation where the vehicle engineer has to make a well balanced compromise between NVH and powertrain performance. The complete powertrain and drive-line system contains engine, clutch, transmission, drive shafts, joints, and wheels present a complex torsional and bending vibration system, and this causes disturbing NVH phenomena.

The gearbox housing encloses all the components of a transmission. These are some of the main functions of a transmission: absorb acting operational forces and moments when gears are engaged, maintain the accurate position of the shafts and gears relative to each other during different operational conditions, provide rigidity and strength to transmission layout and insulate and dampen gear noises.

The transmission in a vehicle is one of the major noise sources and this noise can be divided into four categories:

- Gear whine
- Rattling/Clattering
- Clonk noise
- Shifting noise.

There are constant developments in the automotive industry to reduce the noise in the form of NVH studies. A sudden torque change in the engine leads to the backlash afflicted components thrashing against one another. The result of this exchange of impulse is a metallic, disturbing noise known as "Clonk Noise". This phenomena occurs when downshifting, park-lock releasing and synchronization of 1st gear, reversing or any kind of sudden force transfer occurrence.

This master thesis is performed in collaboration with the engineering company CEVT AB (China Euro Vehicle Technology AB) and is focusing on the simulation and measurement of dual clutch transmission (DCT), and in particular to understand the clonk behavior.

1.1 Background

The base design of a DCT transmission is in reality two manual transmissions in one housing with two separate clutches, however, the way in which the transmission is operated by the driver is mostly the same as an automatic transmission except most DCT also has the ability to allow the driver to manually shift gears in semi-automatic mode.

Different dynamic pulses/forces arise during the release of the park lock and engaging first gear or reverse. These dynamic pulses can also be caused by the clashing of gears when rotational speed changes during the synchronization process, and originate clonk noise in the transmission.

Clonk noise as other transmission noises affects in a negative way to the overall quality perception of the transmission, powertrain and vehicle in general. A further understanding on how the clonk noise is radiated from the transmission structure so that countermeasures can be implemented to attenuate the effects of clonk noise is needed.

1.2 Objective

- Use an existing CAE model to create a simulation model with different methods of analysis and get the velocities needed for an acoustic model
- Develop an acoustic model by using FEM and IEM to determine the sound (pressure, power, directivity) radiating from the transmission's surfaces
- Validate the simulation model with measurements of a physical model.

1.3 Limitation

- The CAE (Computer-aided Engineering) model was already available, extra parts (oil pump, electric control etc.) of the structure is removed, only the gear case and clutch case are studied further;
- The thesis is working on getting a simulation model to work with structural and acoustical simulations;
- Clonk noise is the priority and thus the study is focused on higher frequency range, $f > 300\text{Hz}$.
- Due to restrictions from the company's policy's, the complete model is not shown, only parts of the transmission.

2

Dual Clutch Transmission (DCT)

This chapter will describe the gearbox components and materials. The acoustic part of the gearbox is also investigated. Dual Clutch Transmission (DCT) were already being developed in the 1940s, and the first DCT for passenger cars went into production in 2003[2]. Typical dual clutch transmissions come with six to seven speeds and a lay-shaft design for trans-axes used in Front-wheel drive (FWD) and Rear-wheel drive (RWD) applications as well as inline configurations. A DCT allows more freedom to change most gear ratios individually with minimum effort, and combines efficiency, sportiness, and comfort, each on the highest levels[3].

2.1 Basic Principle

The main principle of a dual clutch transmission is based on the idea of two independent sub-gearboxes each connected to the engine via its own clutch. One of the sub-gearbox contains the odd gears (1, 3, 5...) and the other one contains even gears (2, 4, 6...)[2]. As it is shown in the Figure 2.1, an example design of a 6-speed DCT in actual, the two sub-gearboxes are not arranged side-by-side, one of the two gearbox input shafts is used as a hollow shaft[2], and one is nested in the other to save space. The main sections with power flow in the figure are listed in Table 2.1.

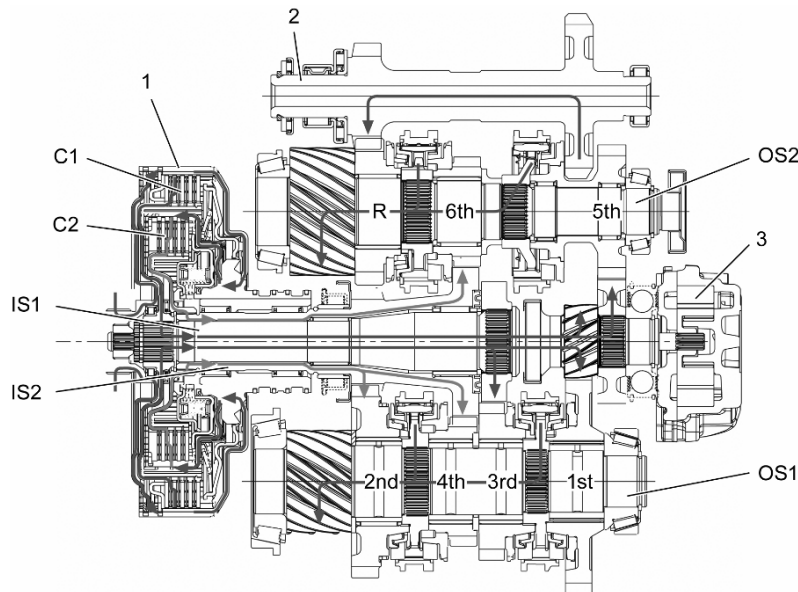


Figure 2.1: Basic diagram of a 6-speed passenger car DCT VW DS[®][4].

Code Name	Component Name
C1	Clutch plate 1
C2	Clutch plate 2
1	Wet-running dual clutch with C1 and C2
2	Reverse idler shaft
3	Oil pump
IS1	Input shaft of sub-gearbox 1 (1st/3rd/5th/R)
IS2	Input shaft of sub-gearbox 2 (2nd/4th/6th)
OS1	Output shaft 1 with output constant pinion
OS2	Output shaft 2 with output constant pinion

Table 2.1: Name of the DCT main sections with power flow

A dual clutch works when the engine drives the outer plate carriers of the clutches C1 and C2 through the dual mass flywheel. A stub shaft spline is used to connect the inner plate carriers of the two clutches to the input shafts of the two sub-gearboxes: sub-gearbox 1 with the internal throughout input shaft IS1 (first, third, fifth and reverse gear) and sub-gearbox 2 with the shorter input shaft IS2 designed as a hollow shaft (second, fourth and sixth gear)[4].

2.2 Control

When gears clash, a wave is transmitted, as described in Chapter 3. It is generated from the engine connection to the clutches of the gearbox, then transfers to the input shaft, and across the gears to end up in the final drive. This pulse creates what is called the "Clonk Noise". This happens when shifting gears or manually shifting between the given modes, Park, Reverse, Neutral, Drive or Semi-automatic shifting, basically a force variation which generates a vibration in the components. The driver uses a joystick to shift between R, N, P, N, D in vertical direction and while driving, semi-automatic shifting is available in horizontal direction. The layout is presented in Figure 2.2.

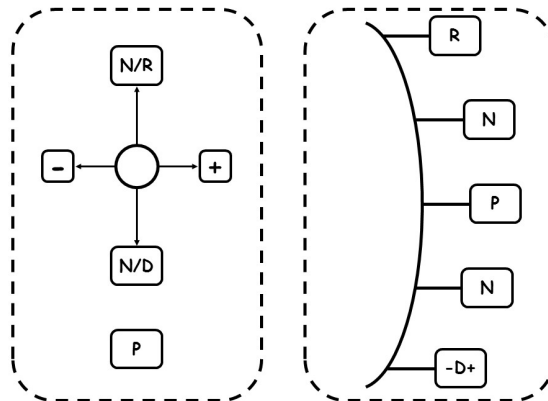


Figure 2.2: Control system layout of shifting modes

2.3 CAE Model

The existing CAE model(Complete) that CEVT has provided is used to create the simulation model, the Complete model is presented in Figure 2.3. The complete model is simulated for three methods while the base model, that only includes the gear- and clutch casing, is simulated for the final two methods. All five methods explained further in Chapter 4. A table for which method is used for which model is presented in Table 2.2.

Method	Complete	Base
Dynamic Implicit	✓	
Free Response	✓	
Forced Response Direct	✓	
Forced Response Modal		✓
Airborne Simulation		✓

Table 2.2: Model used for the methods

The complete model includes most of the components attached to the gearbox except the cables and it is empty inside. A physical model of the base model exists, and is measured in Chapter 5. To validate the simulation, the same base model had to be simulated, and this resulted in removing all the attached components in the complete model. The casings of clutches and gears are the only two parts that is included in the base model.

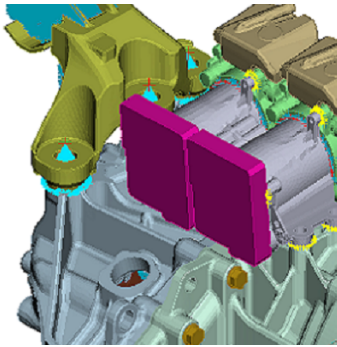


Figure 2.3: Complete model

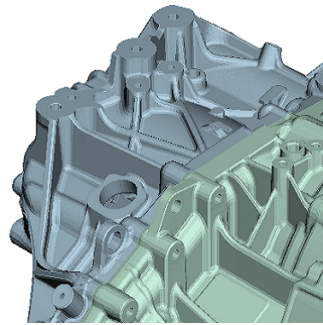


Figure 2.4: Base model

The base is an Aluminum alloy with Silicon and Magnesium. The two cases are connected with steel bolts. The properties of the base are listed in Table 2.3, the structure is built with solids and meshed with CTETRA (Four-Sided Solid Element Connection: Defines the connections of a four-sided isoparametric solid element with four to ten grid points.) elements.

Material	Density	Young's Modules	Poisson's Ratio
AlSi10Mg	2.83 g/cm^3	71.00 GPa	0.33
Steel	7.85 g/cm^3	210.00 GPa	0.30

Table 2.3: Material properties of the casing

2.4 Clonk Noise and Propagation

The transmission in the powertrain chain often generates a high proportion of noise. During the beginning loading of components (gearwheels, shaft-hub connection etc.) with clearance the knocking noise might occur. As a reaction to the sudden load change, there is a low-frequency longitudinal vibration (about 2 - 8 Hz) of the vehicle, in addition to that, at higher frequency (about 300 - 8000 Hz) a metallic-sounding noise will occur as the "clonk" noise, that arise when the flanks of active components knock against each other[5].

A force variation which generates a vibration in the components (the flanks of the gearwheels) is the main reason of noise generating from the gears, then the vibration is transmitted to the surrounding structure. The airborne noise is produced only when the vibrations excites the external panels, the noise level and characters are influenced in various approaches by the transmissions path before it reaches the ear of the driver. Figure 2.5 indicates the propagation path.

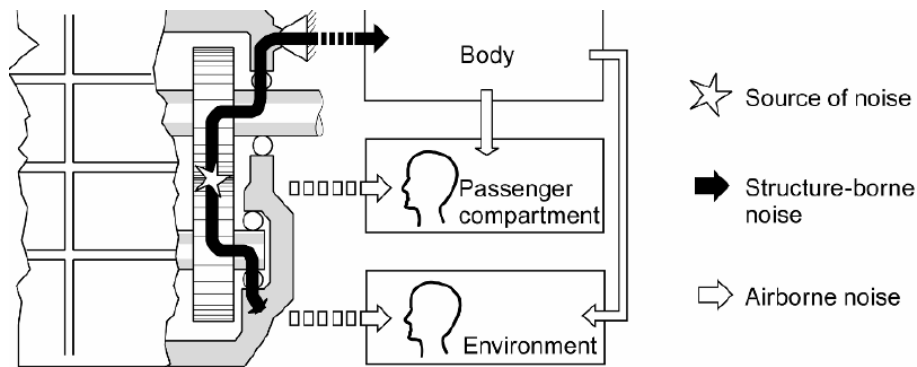


Figure 2.5: Propagation path of airborne and structure borne noise [6]

Though there are high noise levels inside a sealed gearbox, this usually does not influence much since the air pressure fluctuations are not powerful enough to excite the housing significantly. The structure-borne noise is transmitted from the vibrations of the gearwheel to the shafts, and through the bearings to the bearing seats connected to the gear box. Thus, the vibrations transmitted to the housing are mainly through the shaft bearings, and the torsional waves of the shafts will excite the housing particularly. Once the excitation frequency is close to the eigenfrequency of the housing, the vibrations are significantly amplified, and high noise levels will occur correspondingly. Finally, part of the noise from the gearbox housing is radiated as airborne noise, and the rest is transmitted as structure-borne sound to the rest of the body through the gearbox mounting[6].

3

Theory

The structural acoustic process can be subdivided into four main stages[7]:

1. Generation
2. Transmission
3. Propagation
4. Radiation.

Since there are three different scenarios for the occurrence of clonk noise:

- Park-lock disengagement (P)
- 1st gear engagement (D)
- Reverse gear engagement (R).

Thus, the generation of sound is in three different gears in the transmission. But all of these three gears are also sitting on top of the same output shaft. This output shaft is held in place with bearings that are directly connected to the housing. This is where the pulse of the gear clash transports until it propagates to the housing, and at certain velocities (above the speed of sound in air), radiation of sound waves occurs. The DCT structure is shown in the previous Chapter 2.

This phenomenon occurs in less than one tenth of a second and the first step is to understand it before simulating it. If it is assumed that the sound is in the higher frequency range then a study of the behavior of the structure at those frequencies can be sufficient. The transmission housing is assumed to keep all the airborne sound that occurs when the gears clash inside, which is negligible, for the IEM simulation.

3.1 Wave Theory

Many different waves exist in solids at low frequencies. And at higher frequencies, the width or thickness of the structure is not small enough when compared to the wavelength, thus, different types of waves are present at the same time.

The process can be explained with "wave patterns"[8] and it is shown in Figure 3.1 with a simple sketch. Where H is the hit of the gears clashing and:

1. Internal Sound Waves
2. Torsional Waves
3. Longitudinal Waves
4. Bending Waves
5. Structure-Borne Sound Radiation.

As mentioned in the previous section, the internal sound waves are not of interest.

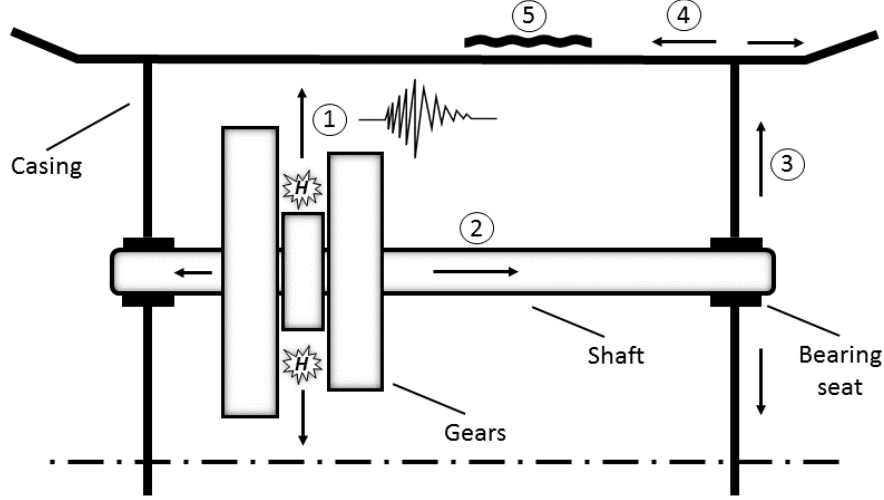


Figure 3.1: Sketch of wave patterns

3.2 Finite Element Method

The Finite Element Method is a common method used in engineering[9]. FEM is basically splitting up the problem into smaller sub-problems (finite elements) with known solutions, similar to how the wave approach works but with more than one dimension of propagation. FEM is used to calculate the surface vibrations of the model[9].

The basic process to solve a problem in FEM is:

1. Define problem as Differential Equations(DE) and Boundary Conditions(BC)
2. Optimize DE for numerical problem
3. Split the problem into smaller sub-problems with known solutions
4. Couple these sub-domains into a system of equations
5. Solve the coupled problem

To optimize the DE, there are two approaches on how this is done:

1. Hamilton's principle/variational approach
2. Weighted residuals/Galerkin's method

Hamilton's principle is only applicable to certain problems and are less commonly used. The weighted residual method can be used for all problems and the structure of the gearbox is complicated thus this method is used.

Meshing the model gives the correct element sizes, basically splits the problem into smaller sub-problems. Meshing is explained in the next section. Coupling these sub-domains into a system of equations results in a discrete FE equations:

$$\underbrace{F_{FEM}(\omega)}_{force\,vector} = \left(\underbrace{K_{FEM}}_{stiffness\,matrix} - \omega^2 \underbrace{M_{FEM}}_{mass\,matrix} \right) \underbrace{\dot{u}(\omega)}_{nodal\,displacement\,vector}, \quad (3.1)$$

where $F_{FEM}(\omega)$ is the force vector depended on ω frequency, K_{FEM} and M_{FEM} represent the stiffness matrix and mass matrix respectively, and $\dot{u}(\omega)$ is the nodal displacement vector.

The last step is solving the equation (3.1), this can be done with different methods:

- Free Response
- Forced Response Direct
- Forced Response Modal
- Dynamic Implicit.

Free response means that the force vector is equal to 0:

$$0 = (K_{FEM} - \omega^2 M_{FEM})u(\omega) , \quad (3.2)$$

and the solutions is given as natural frequencies ω_n and mode shapes Φ_n :

$$(K_{FEM} - \omega_n^2 M_{FEM})\Phi_n(\omega) = 0 . \quad (3.3)$$

The eigenvalues is calculated using the determinant with:

$$\det(K_{FEM} - \omega_n^2 M_{FEM}) = 0 . \quad (3.4)$$

The forced response can be solved with two possible strategies, direct and modal, each has their own advantages and disadvantages. Direct solutions can be done with matrix inversion to the DE equations for each frequency:

$$u(\omega) = (K_{FEM} - \omega^2 M_{FEM})^{-1} F_{FEM}(\omega) . \quad (3.5)$$

And modal solutions can be done using the natural frequencies and mode shapes from the free response solutions with added damping and force:

$$u(\omega) = \sum_{n=1}^N \frac{\Phi_n^T F(\omega)}{(\omega_n^2 - \omega^2) + i\eta_n \omega_n^2} \Phi_n . \quad (3.6)$$

The Dynamic implicit is a method that solves the problem in the time domain. Each method is simulated, presented and explained further in Chapter 4.

3.2.1 Frequency Limitation

The frequency limit for the finite element method is dependent on the element type and the mesh size that is used. Provided that a quadratic shape function is used (with a node between every corner-node of a triangular mesh element) the upper frequency range can be roughly estimated from the mesh size. If one wants to be certain that the displacements in the material from waves are modelled correctly there should fit approximately one sixth of a wavelength between two nodes. The largest side length of a mesh element can be extracted and if this measure, a , corresponds to a sixth of a wavelength we have that $3a = \lambda$. In our model the maximum element length is 10 mm, this means:

$$\begin{aligned} \lambda &= 3 \cdot 0.01m = 0.03 , \\ f_{max} &= c \cdot \lambda = \frac{343}{0.03} = 11435 \text{ Hz} . \end{aligned} \quad (3.7)$$

3.3 Infinite Element Method

Infinite element computations are very efficient for predicting the vibro-acoustic response and sensitivities of a vibrating structure for an exterior acoustic domain[10]. Infinite elements are one of the specific finite elements that the units are extended to infinity in geometry, also the infinite element method is a modification and supplement of finite element method in solving non-boundary problems.

A comparison between FEM and IFM is shown in the Table 3.1 below.

	Advantages	Disadvantages
FEM	<ul style="list-style-type: none"> - Non-local boundary conditions - Can be applied for non-convex geometries 	<ul style="list-style-type: none"> - Full, frequency dependent system matrices
IEM	<ul style="list-style-type: none"> - Far field results obtained straightforwardly - Frequency independent system matrices 	<ul style="list-style-type: none"> - Can only be applied for convex geometries

Table 3.1: Comparison between FEM and IEM

Infinite elements are based on the Helmholtz differential equation, applied to semi-infinite sectors of the domain that are exterior to an artificial boundary surrounding the structure, with acoustic finite elements between the structure and the boundary[11]. Infinite elements are always combined with acoustic finite elements, and acoustic finite elements are also used to model the propagation in the near field of the source while the acoustic infinite elements are used to model the radiation in the far field. A typical example of such a geometry is shown in Figure 3.2 for a two-dimensional case.

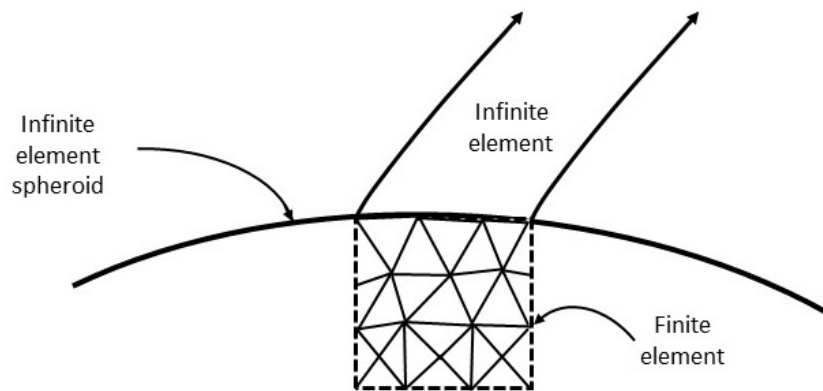


Figure 3.2: Geometry at interface between infinite and finite elements

In order to use the IEM to the analysis of an acoustical problem, such like a gearbox, it is necessary to define a convex envelope surrounding the object in the first step, as it is shown in Figure 3.3 when considering a two-dimensional case. The volume between the object and the convex envelope is then meshed with finite elements, and infinite elements are defined on the surface of the convex envelope[12].

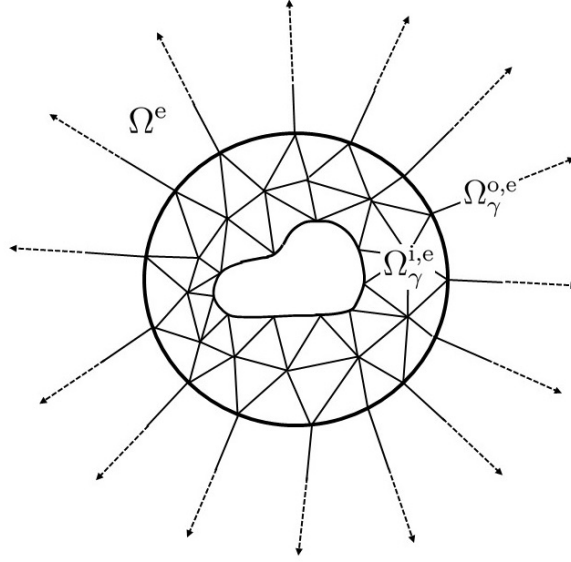


Figure 3.3: Mesh around the object ($\Omega^e = \Omega_\gamma^{i,e} \cup \Omega_\gamma^{o,e}$).

In this problem that is shown in Figure 3.3, an unbounded domain is defined as Ω^e , a bounded domain $\Omega_\gamma^{i,e}$ is defined as a truncation of the Ω^e as:

$$\Omega_\gamma^{i,e} = \Omega^e \cap \{x \in \mathbb{R}^3; |x| < \gamma\} , \quad (3.8)$$

the artificial boundary is introduced as a sphere S_γ , and γ is the radius of S_γ . While the bounded domain $\Omega_\gamma^{i,e}$ is meshed with finite elements, and the exterior of the domain $\Omega_\gamma^{i,e}$ is defined as $\Omega_\gamma^{o,e}$:

$$\Omega_\gamma^{o,e} = \{x \in \mathbb{R}^3; \gamma < |x|\} , \quad (3.9)$$

and $\Omega_\gamma^{o,e}$ is meshed with infinite elements. The optimal distance between the object and the artificial boundary S_γ depends on the order of the infinite elements considered[13].

Both the acoustic finite and infinite element is air during the simulation, with the properties given in Table 3.2

Material	Density	Speed of Sound
Air	$1.18g/cm^3$	$343m/s$

Table 3.2: Element properties in acoustics

3.4 Equivalent Radiated Power

Equivalent radiated power, known as "ERP", is also applied to our simulation model. The simulations outputs the structure velocity on the surface. As the surface area is known, thus, the equivalent radiated power can be calculated. This is a much more efficient method than the infinite element method if one wants to know, where does most sound radiate on the structure so that countermeasures can be implemented to reduce it[14].

The underlying theory starts with the definition of complex intensity (\underline{I}) in the frequency domain:

$$\underline{I} = \underline{p}\underline{v} \ , \quad (3.10)$$

where \underline{p} is complex pressure and \underline{v} is complex velocity. If the intensity is integrated with the an area with explicit spatial orientation, the acoustic power can be calculated:

$$P = \text{Re} \left\{ \int_A \underline{I} d\vec{A} \right\} . \quad (3.11)$$

This means that the acoustic power can only be calculated if pressure and spatial particle velocity are known for each node. This is not possible without the infinite element method, therefore the ERP calculation makes some simplifications. It is assumed that a planar and rigid radiating surface and only plane wave is emitted. A plane wave is only propagating in one dimension and it can be shown that sound pressure and particle velocity are in phase. This results in the impedance being:

$$Z = \frac{\hat{p}}{\hat{v}} = \rho_F c_F . \quad (3.12)$$

The impedance is real with density of the fluid, in our case air ρ_F , sound velocity c_F and the amplitudes of sound pressure \hat{p} and particle velocity \hat{v} . Using these formulas and with the assumptions that air moves at the same speed as the structure node velocities:

$$v_{S,n} = v_F . \quad (3.13)$$

The ERP formula follows as:

$$ERP = \rho_F c_F \int_A |v_{S,n}|^2 dA . \quad (3.14)$$

The assumptions made are only valid up to the first natural frequency is reached, at higher frequencies the movement of the structure has different phase relations, so acoustic short-circuits appear as well as directivity of radiation appears. This method is an overestimation, just an approximation, but it is regularly used in early phases of product developments. And this can be expressed in dB:

$$ERP_{dB} = 10 \log_{10} \left(\frac{ERP}{ERP_{ref}} \right) , \quad (3.15)$$

where the ERP_{ref} is the reference value of the standard 10^{-12}W .

4

Simulation Methods and Results

This chapter is focusing on the procedure of the simulation methods. The advantages and disadvantages of each method together with personal thoughts and discussions. The complete and base model described in Chapter 2 are used. A simulation procedure is processed in three steps:

1. Pre-Process: Setting up a simulation model with the chosen method, *ANSA*® and *Actran*® are used to Pre-Process.
2. Solver: Solving the equations is done with a solver. Three different solvers are used, *Abaqus*®, *Nastran*® and *Actran*®.
3. Post-Process: *META*® and *PLTViewer*® are used for Post-Processing the results.

4.1 Dynamic Implicit

The initial plan for simulating was to use the Dynamic Implicit Method. This method would be optimal for simulating the clonk phenomenon since it calculates in the time domain. The software used for this method is *Abaqus*®. A setup for this simulation needs to satisfy some parameters, boundary conditions, hits, contacts etc.

A problem is dynamic when the inertial forces are significant and vary rapidly in time, clonk noise is a result of a dynamic force acting on the gears. The dynamic equilibrium equation is:

$$P - I = Mu(t) , \quad (4.1)$$

where,

M : Mass matrix

P : External force vector

I : Internal force vector

u, \dot{u}, \ddot{u} : Displacement, velocity, and acceleration vectors.

For *linear* problems:

$$\mathbf{I} = \mathbf{C}\dot{u}(t) + \mathbf{K}u(t) , \quad (4.2)$$

where:

C : Damping matrix

K : Stiffness matrix.

Solving a *nonlinear* dynamic problem requires the integration of the equation of motion. Discretization in both space and time, and direct-integration in FEM.

When the inertial force is small enough, the equation reduces to the static form of equilibrium. The dynamic implicit is a very resource intensive simulation method. The complete model was used to create the simulation with all parts available and is shown in Figure 4.1.

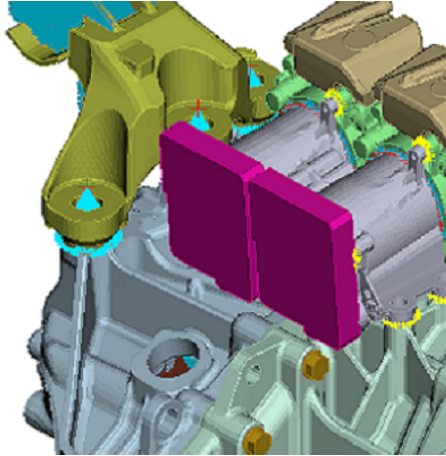


Figure 4.1: Complete model used to create simulation

Starting from the boundary conditions, only one boundary conditions were used for this simulation. The gearbox is mounted to the engine from the front side. Locking the front side of the gearbox 1, 2, 3 directions, this simulates that the gearbox front, doesn't have displacements in the X, Y and Z directions. The boundary conditions are displayed in Figure 4.2 in black.

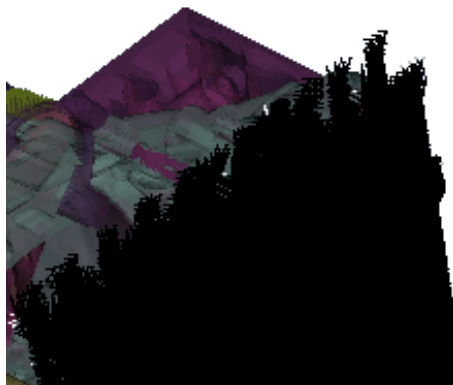


Figure 4.2: Boundary condition used in simulation

The complete model is an assembly of different parts, and these parts have contacts with each other. This is achieved with *TIE* contacts, it *ties* two surfaces forming a contact pair together for the duration of a simulation. Nineteen contact groups are

available in this model, including the bolts. The contacts are marked with red and blue color and are displayed in Figure 4.3.

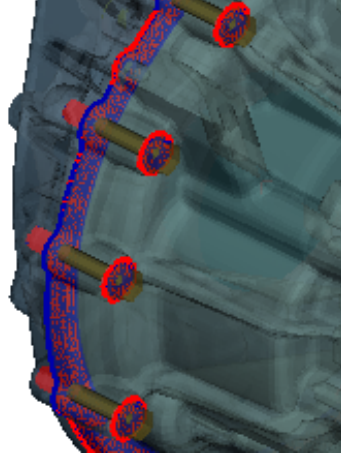


Figure 4.3: Groups of contact

Constraints are used to partially or fully eliminate degrees of freedom of a group of nodes and couple their motion to the motion of a master node. The constraints of the complete model are marked with three color: yellow, light blue and purple. These represent respectively to:

- MPC: Multi-Point Constraint is used to specify linear or nonlinear constraints between nodes, one is shown for the inside of the clutch casing
- Distributing Coupling: applies the constraint in an average sense but using weight factors specified at the coupling nodes. Coupling constraints are used to represent bearings and the master node is set in the center
- Kinematic Coupling: limits the motion of a group of nodes to the rigid body motion defined by a reference node, used on the electric components on top of the gearbox.

The constraints are displaced in Figure 4.4 with the mentioned colors.

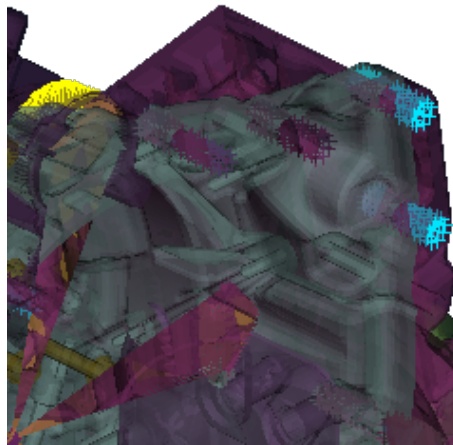


Figure 4.4: Groups of constraints

An instantaneous *Load* on the structure was applied at the location of one of the

bearings. 5 *Newton* in the positive Z-direction as a *CLOAD*, concentrated load, is applied to a node. The load is displayed in Figure 4.5. The position of the *Load* was randomly selected to test the simulation method.



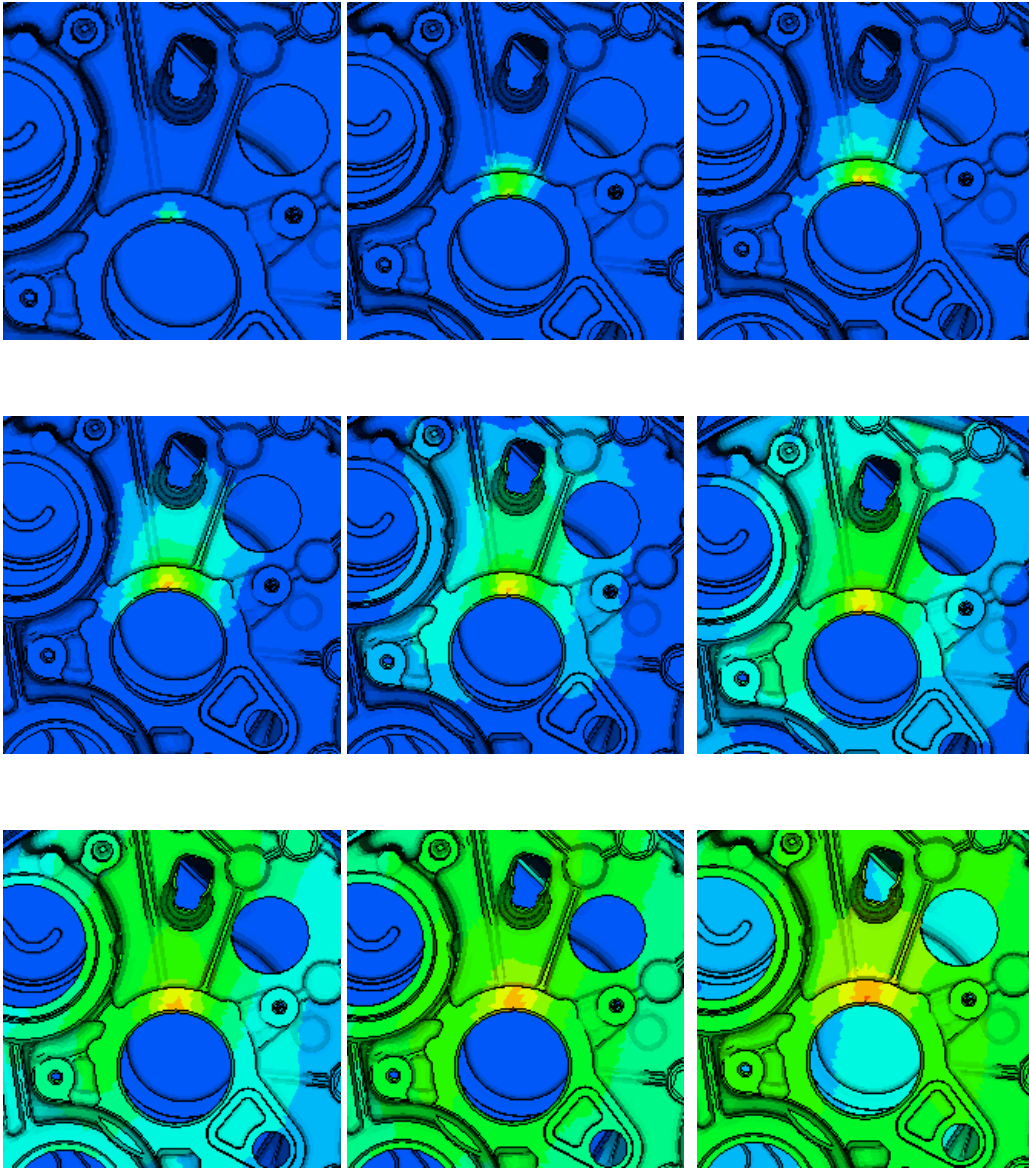
Figure 4.5: Vertical Hit

After implementing all the needed parameters, the solver for the dynamic implicit method was chosen with the parameters shown in Table 4.1. This was in accordance with the expected time period for clonk to occur, TIMEPER, the time period is set to 0.01 seconds. TIMEINC is how much in time the results should be printed in each increment. MININC is the minimum increment that the solver should use, 0 means that the computer calculates the appropriate minimum increment. MAXINC is the maximum increment that the solver uses, it is set to 0.001 seconds, the solution takes longer time the less this step is set, a good start for this calculation is the chosen value.

TIMEINC	TIMEPER	MININC	MAXINC
0.004	0.01	0.000	0.001

Table 4.1: Step parameters

The simulation worked, but not as expected. It could only solve a very small amount of time period and not as far as the setting in Table 4.1. The reason for this is the mesh size of the model, the large number of elements resulted in the solver crashing after solving only 0.86 *milliseconds*. The results are presented in the following ten figures where only the base is shown to visualize the inner displacements.



Since this simulation wasn't able to calculate the required time period and the time for this calculation took more than 24 hours, any further development on this method was aborted.

4.2 Free Response

The free response is the characterization of the behavior of the structure at certain modes. The free response is the Equations 3.2, 3.3 and 3.4 solved. Mode shapes up to a certain frequency were solved, since the higher frequencies are of interest, the range was set accordingly and the computation time reduced. The free response method helps to determine the modes of vibrations and the frequencies at which these modes are triggered. It doesn't give any information about the real deformation that an excitation of one of the modes is actually cause. It calculates the eigenvalues and the eigenfrequencies at the given frequency range. The modes of

vibration are theoretically infinite but the ones that will lead to the largest displacements are generally wanted to locate[15].

One of the mode shapes of interest was found at 2467 Hz. Here, a bright red point is located on the structure, shown in Figure 4.6. This shows that at that frequency, the structure displacement is significant at that location. Further studies at that frequency are conducted in the forced response method.

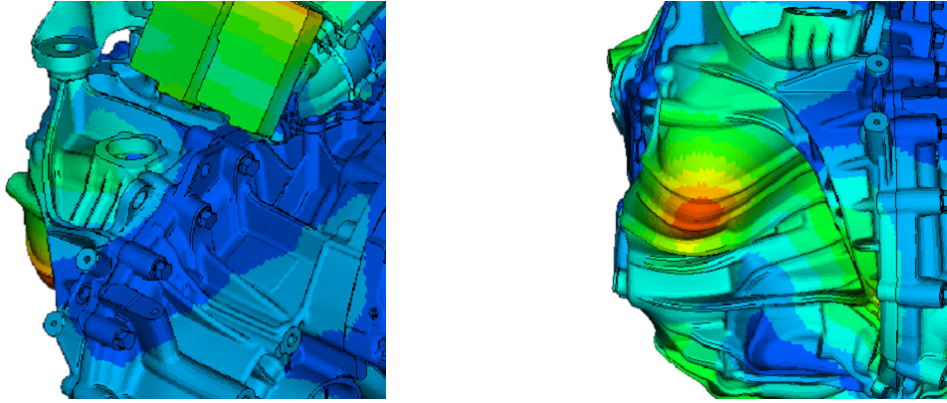


Figure 4.6: Mode shapes at 2467Hz

Now that we have found some modes that resonate the gearbox, we need to excite them with a load, solving a forced response analysis to get the real displacements and accelerations of the structure vibrations.

4.3 Direct Method versus Modal Method

When doing a forced response simulation, there are two ways to approach the problem, depending on which models are wanted to solve and the computation time available. The direct method is more accurate but it takes longer time to solve, which is proportional to the complexity of the model. It is usually used for small models that have few excitation frequencies, also since it doesn't require damping, it can obtain a more accurate result. However, in this case the model is big and with lots of elements, and it requires many excitation frequencies to locate the clonk frequency. To simulate clonk, many frequencies is needed for both approaches, but once you have the eigenfrequencies, the modal approach can be significantly faster. Both methods are tested and a summary is presented in Table 4.2 for the approaches [16].

Model Types	Modal	Direct
Small Model		✓
Large Model	✓	
Few Excitation Frequencies		✓
Many Excitation Frequencies	✓	
High Frequency Excitation		✓
Non-modal Damping		✓
Higher Accuracy		✓

Table 4.2: Modal vs Direct method

The results obtained from a frequency response analysis includes the displacements, velocities and accelerations of grid points. The forces and stresses of the elements could also be of importance. While the direct method solves the coupling equations of motion in terms of forcing frequency, the modal method utilizes the mode shapes of the structure to reduce and uncouple the equations of motion.

4.3.1 Forced Response, Direct Method

The Direct Method is the Equation 3.5 solved. A change in the load was applied with this simulation. A moment of 1 Nm in the Y-Direction for all four bearing positions for the output shafts was applied. This was done to roughly estimate a clonk scenario. The loads can be seen in Figure 4.7. No other changes to the model was applied and the software *Abaqus*® was used as the solver.

**Figure 4.7:** Torsional Hit

As the solver took one hour to calculate only two frequencies (4 kHz and 5 kHz), which is not a reasonable computation time, thus this method was not studied further. The result for 4 kHz is presented in Figure 4.8:

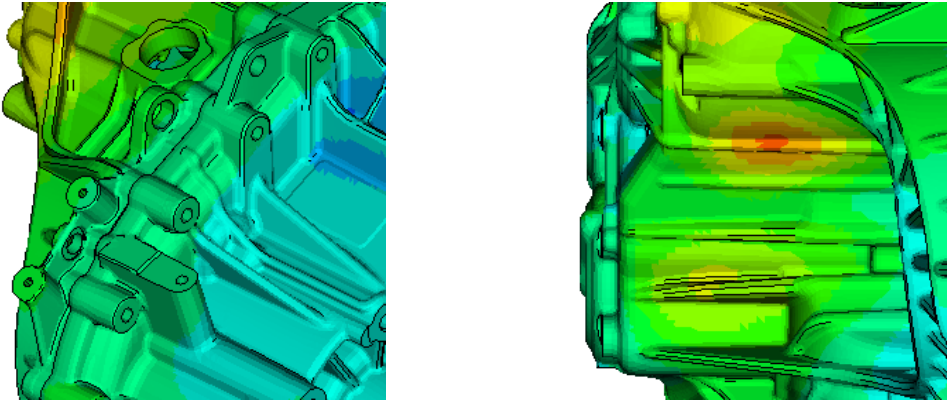


Figure 4.8: Mode shapes at 4000Hz

The direct method is useful for computing structural vibration simulations, but to calculate the results for a airborne noise simulation, another software was required.

4.3.2 Forced Response, Modal Method

The Modal Method is the Equation 3.6 solved. It uses the mode shapes of the structure to reduce the size, uncouple the equations of motion, and makes the numerical solution more efficient[16]. The mode shapes are typically computed as part of the characterization of the structure, modal frequency response is a natural extension of a normal modes analysis. This method is more computationally efficient than the direct method.

The analysis was solved with *Nastran*[®] as SOL111. This was because, the simulation results in this software is needed for the airborne noise simulation.

The gearbox was reduced to its base model for the modal analysis, which is presented in Figure 4.9. The base model was used because the measurements are made of the physical base model and the solutions of the simulation are compared.

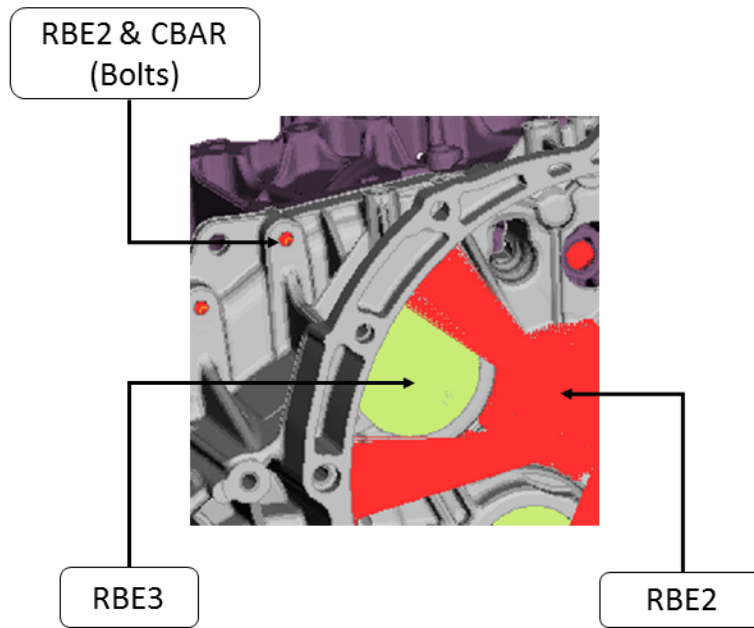


Figure 4.9: Base Model

All *Contacts*, *Constraints* and *Loads* had to be removed, since they are properties in another software, *Abaqus*[®], and the software we are using, *Nastran*[®], for the modal approach, doesn't understand those properties.

The boundary conditions that was applied previously on the front part was also removed. This is was done since, when measurements are performed, the gearbox is planned to be hanging freely.

A way to connect the casings in *Nastran*[®] is to create bolts by using:

- **CBAR**, Simple Beam Elements, Defines the steel body of a bolt
- **RBE2**, Rigid Body Elements 2, Defines an arbitrary number of grid points locked at a single grid point.

For the bearings position, **RBE3** is used. It defines the motion at a reference grid point as the weighted average of the motions at a set of other grid points.

The difference between **RBE2** and **RBE3** can be seen by the Figures 4.10 and 4.11.

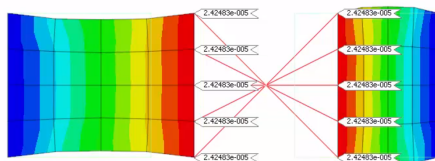


Figure 4.10: RBE2

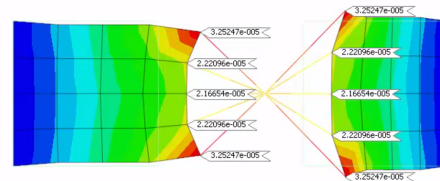


Figure 4.11: RBE3

To define two dynamic loading cases of the form:

$$P(f) = AB(f)e^{i\Phi(f)} , \quad (4.3)$$

where A represents to **DAREA** and it is set as shown in Table 4.3, the hit is on a node in **Fz** direction with the scale factor of 1.

HIT	SID	by	P	C	A	T	TH
HITCase	2	node	1291048	Fz	1		
HITOutput	3	node	1322252	Fz	1		

Table 4.3: DAREA

And B represents **RLOAD2**, and it is set as shown in Table 4.4, which shows what kind of excitation it is, there is a choice between load, displacement, velocity and acceleration. The structure is to be hit by a hammer during the measurement thus a load is applied on the structure in the simulation, and -1 *Newton* in **Fz** direction across all frequencies (RB).

HIT	KEYWORD	SID	EXCITED	TB/RB	RB	TYPE
HITCase	RLOAD2	3	2	RB	-1	0 Load
HITOutput	RLOAD2	3	3	RB	-1	0 Load

Table 4.4: RLOAD

The two loading cases are presented in Figure 4.12 and Figure 4.13:



Figure 4.12: Load case "HITCase"

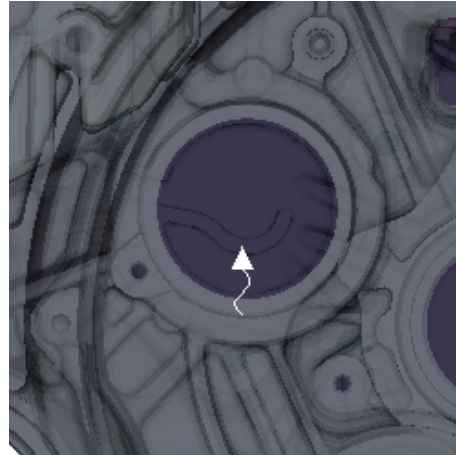


Figure 4.13: Load case "HITOutput"

It is important to select the frequency at which the solution is to be performed correctly. Each specified frequency results in an independent solution at the specified excitation frequency. **FREQ4** is used for this, it defines excitation frequencies using a spread about each normal mode within a range. As shown in the Table 4.5, **F1** and **F2** are respectively lower and upper bound of modal frequency range. **FREQ4**

chooses ten equally spaced frequencies across a frequency band of $0.7 f_N$ to $1.3 f_N$ for each natural frequency between 1000 Hz and 4000 Hz.

Type	SID	F1	F2	FSPD	NFM
FREQ4	1	1000	4000	0.3	10

Table 4.5: Frequency Range

The eigenfrequency for a free case is calculated before the calculation of the forced case. The eigenfrequency calculation is chosen less than the minimum excitation frequency and more than the maximum. For this problem the eigenfrequency range was selected between 0 Hz and 5000 Hz.

In literature the damping (loss) factor is given as $\eta = 10^{-2}$ for constructions of several big (thick) and small (thin) elements like a gearbox[8]. The damping factor 0.01 was used in calculation. The real damping factor is calculated using the half-power bandwidth method after doing the measurements and applied to the simulation.

Results are plotted in Figure 4.14 and Figure 4.15, the "weak" point that was shown in Figure 4.6, was excited at 2500 Hz for the HITOutput but almost nothing is seen on the HITCase.

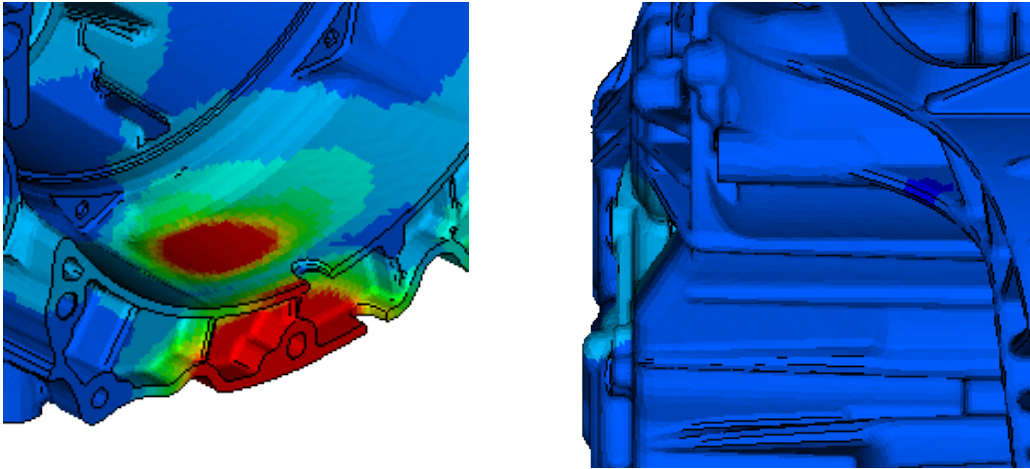


Figure 4.14: "HITCase", Isometric and Left View, at 2500 Hz

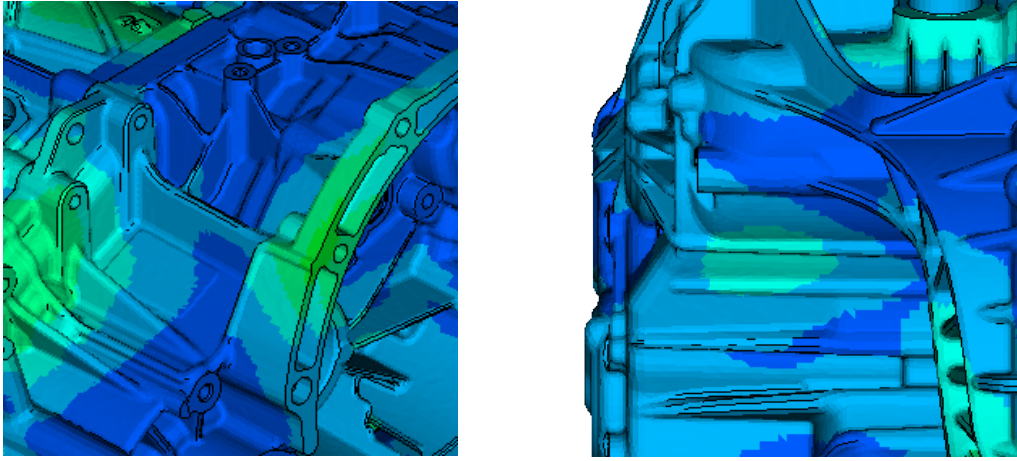


Figure 4.15: "HITOutput", Isometric and Left View, at 2500 Hz

4.4 Infinite Element Analysis

The Infinite Element Method(IEM) is used to calculate sound radiation outside the gearbox, the implementation strategy is shown in Figure 4.16. The pre-processing of acoustic analysis is handled in *ANSA*[®], and the post-processing analysis is tried to be solved by using *Actran*[®]. Unfortunately, *Actran*[®] was not available to use until nearly the end of out thesis, and due to the time limit, the solving and post-processing was not completed. However, the initial ideas of simulation in *Actran*[®] are introduced in this section.

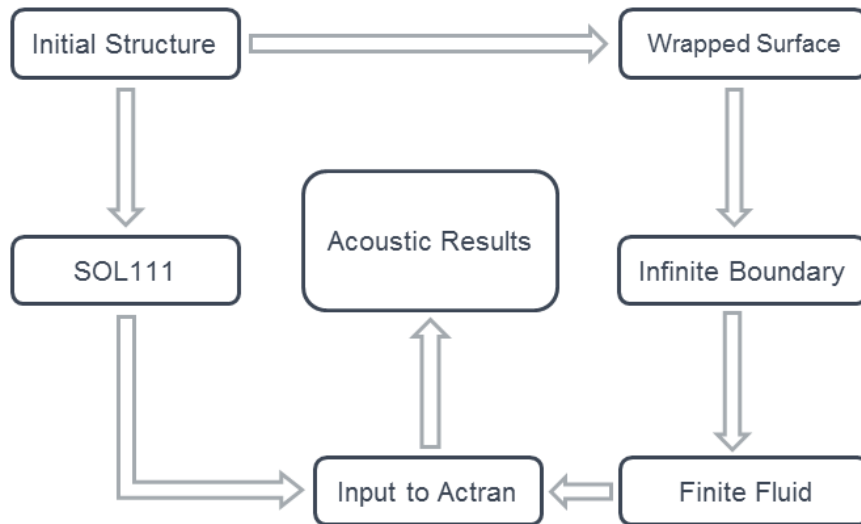


Figure 4.16: Strategy of IEM

4.4.1 Acoustic Model Pre-Processing

The Base Model is shown in Figure 2.4, which has the same setup as the model in the FEM analysis, with mesh type "*trias*" for 2D shell and "*tetras*" for 3D volume.

To solve the exterior acoustic analysis in *Actran*®, one of the most important steps is to have the Boundary Condition results on all of the nodes from the structure in the .op2 format, which is what we have calculated from the *Nastran*® (SOL111 Forced Modal Response Analysis). The meshing function in *ANSA*® pre-processing was used to create the wrapped mesh needed for analyzing exterior noise and radiation characteristics of the structure.

Large openings of the gearbox are closed before wrapping to improve the meshing quality, the wrapped structure with smooth outer surface is shown in Figure 4.17. In the same time, *ANSA*® will automatically create a new "Default PSHELL Property" and assign it to the created warp elements. The *Nastran*® calculation result from the .op2 file is projected in *Actran*® on this surface, which comprises of the boundary conditions, as so-called BC Mesh.

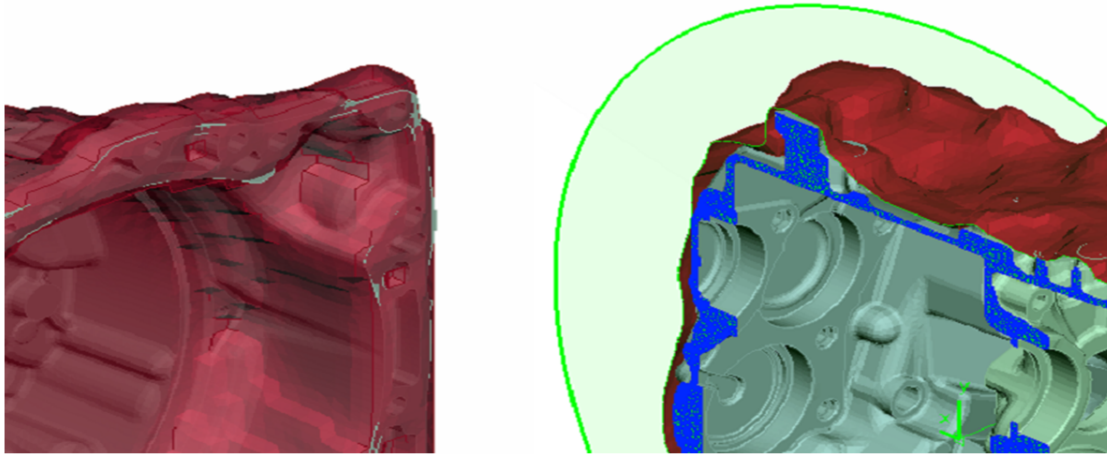


Figure 4.17: Wrapped Surface

Once the wrapped mesh is created, the next step is to create an outer boundary (a infinite surface to support the non-reflective boundary condition), which will enclose the acoustic cavity mesh. The build-in standard surface features is used to create a sphere as the infinite area. The center point is created by using "Create COG Coord./3D Point" feature, and the radius is chosen to be 800 *mm* according to conditions: the ellipsoid fully contains the acoustic sources[17] and the distance between wrapped surface and infinite surface should be larger than one wavelength. The structure with the infinite surface mesh is shown in Figure 4.18.

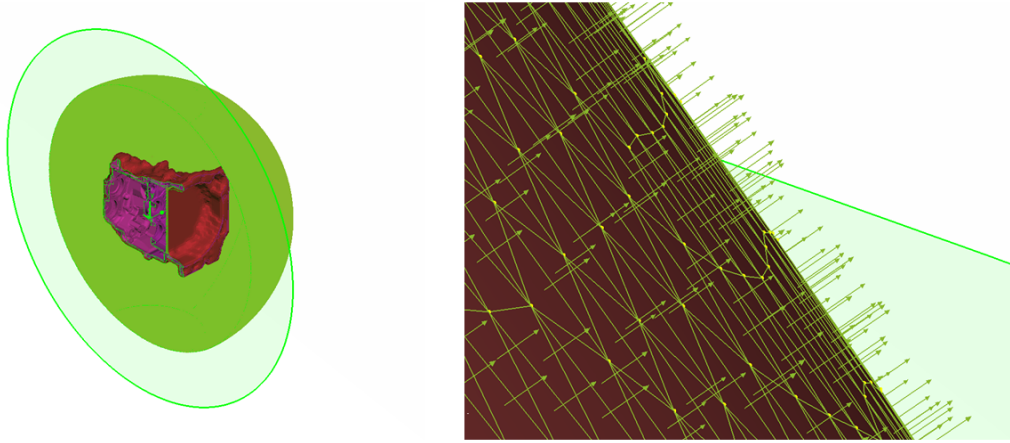


Figure 4.18: Infinite Domain

After the wrapped area and the infinite surface are created, next step is to create FEM volume mesh between the boundaries. The volume entities are detected by using the function "VOLUME MESH > VOLUMES > DEFINE", select the volume which has two shell meshes as boundaries from the "VOLUME" list and "REMESH" the volume with "Tetra Rapid" mesh type. Finally, the resulting volume mesh between the smooth wrap mesh and the outer shell mesh is created, as it is shown in Figure 4.19, which represents the finite area in the analysis.

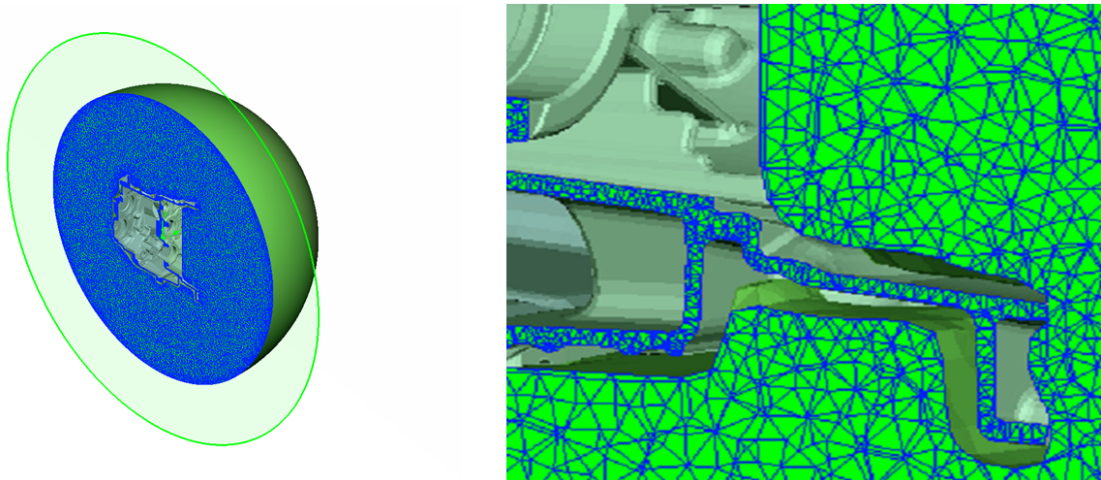


Figure 4.19: Finite Fluid

It should be noticed that there is a relation between the size of the finite element domain relative to the size of the acoustic sources on one side, and the infinite elements' radial interpolation order on the other side[17]. For instance, if the FE domain is small in size then the sound field in the IE domain usually use a higher radial interpolation order. Conversely, if the FE domain is larger then the sound field in the IE domain, it can make use of a lower radial interpolation order. As the element size must be small enough to capture the smallest acoustic wavelength ($\lambda = c/f$) and the small fluctuations that are very close to the structure, in this case, the FE domain is large, so the interpolation order in IE domain is relatively small,

which is chosen to be 15 in the following analysis. However, the way to calculate the interpolation value correctly was not found during this thesis.

The final acoustic model is presented in Figure 4.20, including all the parts needed for an acoustic model.

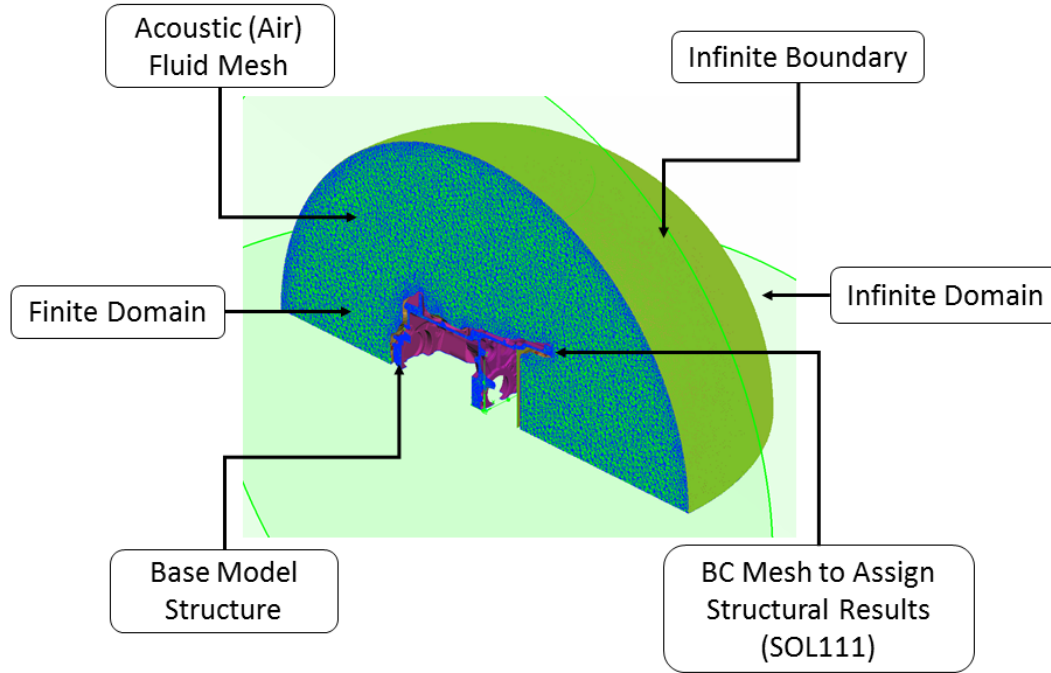


Figure 4.20: Total Acoustic Model

4.4.2 RADACT Interface

Before running the model simulation in Actran, there is a interface embedded in ANSA[®] named RADACT, which is a non GUI wizard tool to create a Actran[®] input file prior to submitting it to the solver. It assigns the respective structural results file and the necessary analysis in the one hand, in the other hand, it can also set up the post-processing parameters. Thus, it was used in order to save simulation time in the thesis.

In the first step, the acoustic fluid mesh, with the respective infinite and wrapped surfaces are imported as an external file. Once the model with the three domains is imported, then the property for the fluid mesh is selected and the physical values for the fluid medium (sound speed and density) are assigned respectively. In the next step, the infinite domain are assigned with the properties created before, which represents the free field condition. After that, the acoustic boundary conditions provided by the structure that hold the forced frequency response results are projected to the wrapped mesh, by using the function **Projection Surface**. In addition, the acoustic field points that represent virtual microphones are imported in as .csv or .txt format. Based on the forced frequency response results that is used to calculate the acoustic radiation, the assignment of the structure and its results are defined.

Before the completion, several analysis parameters are defined also, such as the frequency range that we are interested in, the solver and the type of analysis. Finally, the export location of the RADACT input file is selected. The procedure of creating the RADACT input file is shown in the Appendix from Figure A.1 to Figure A.8 and the final structure of the RADACT is also attached to the Appendix A "RADACT Input File".

4.4.3 Acoustic Model Post-Process

The post-processing of the acoustic model was intended to be handled in *PLTViewer*[®], that is part of *Actran*[®]. Virtual microphones can be located anywhere around the structure model to compute the directivity and the sound pressure levels. The computation of the radiation sound power can be calculated by using multiple control surfaces. *Actran*[®] has a function to automatically define the field points locations according to the standard **ISO 3744**[18]. The results can be inputted as `.plt` file into the *PLTViewer*[®], where the radiated power and directivity can be plotted. Whereas the *Actran*[®] calculation was not completed, so the post-processing in *PLTViewer*[®] cannot be implemented. However, in order to obtain the radiated power, another approach was conducted, the Equivalent Radiated Power(ERP) method.

4.5 ERP Method

The Equivalent Radiated Power (ERP) can be calculated from the structure velocities. This is achieved by creating a skin or shell on the outer layer of the gearbox. The skin is presented in Figure 4.21.

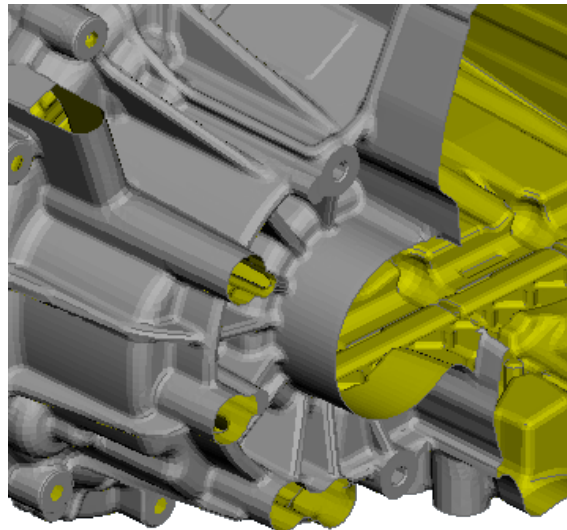


Figure 4.21: ERP Panel, shell meshed with CTRIA6 elements

The skin can be split into smaller parts and this can give a better overview of where most of the sound is radiated. The thesis is only focusing on simulation and

not improvement thus only one total outer surface of the gearbox is created to get the total ERP values of the gearbox. The ERP is calculated alongside the forced response modal analysis, but needed a slight change to get a broader ERP results, where the frequency range was linear with step-size $\Delta = 5$ Hz and starting at 500 Hz with 1000 steps, as shown in Table 4.6.

Type	SID	f_{start}	Δf	NDF
FREQ1	1	500.0	5.0	1000.0

Table 4.6: ERP calculation type and frequency range

The results we got from the ERP calculations are presented in the Figure 4.22. As it is shown in the figure below, "HITCASE" and "HITOUTPUT" represents the load hit on the casing and output shaft respectively.

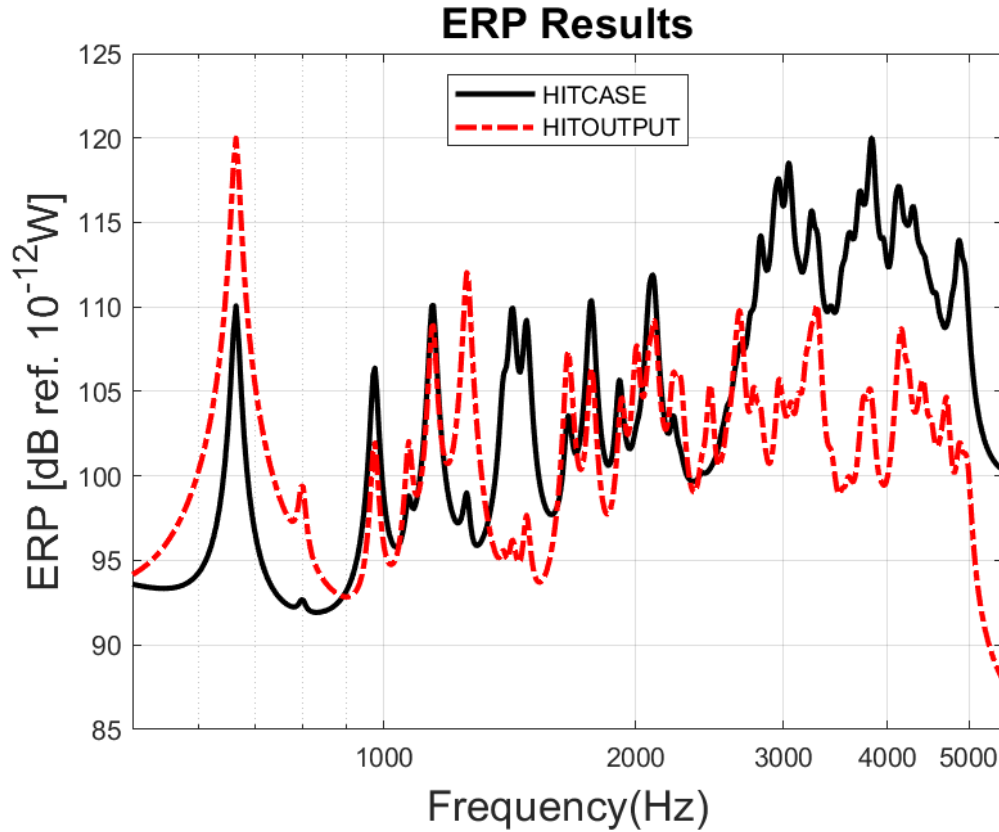


Figure 4.22: ERP results with original properties

In the lower frequency range, from 500 Hz to 900 Hz, the "HITOUTPUT" ERP values are higher than the "HITCASE" values, and they share the peaks at those frequencies. After, there are fluctuations of the results, and when frequency rise up to 2800 Hz, the ERP values for hitting the casing are much higher than the hit on the output shaft position.

5

Measurement

Hammer impact test was implemented to validate and correlate the simulation results. The goals of the measurements include structural vibration and airborne noise radiation.

Measurements are realized with guidelines of Basic Vibration Measurements[19]. The measurements took place on April, 23rd 2018 in the building of the Division of Applied Acoustics at Chalmers University of Technology, Sven Hultins Gata 6, 412 96 Göteborg, Sweden.

5.1 Equipment

The equipment used in measurements is described in Table 5.1. The microphones are calibrated before measurements, the tolerance of deviation is 0.3 dB.

Equipment	Model	Purpose
Accelerometers	B&K 4393V	Measure Vibration
Charge Condition Amplifier	B&K Type 2635	Amplify signal
Force Transducer	B&K 8200	Measure Input force
Microphones	PCB Piezotronics 378B02	Measure Sound

Table 5.1: Equipment used in the measurements

The accelerometer has a reference sensitivity of 0.309 pC/ms^{-2} , lower frequency limit of 16.5 Hz and a mounted resonance frequency of 55 kHz. The weight of the accelerometer is 2.4 g. It has the right properties for our measurement, the resonance frequency is not close to the frequencies we are interested in. The amplifiers has high-pass filters that is set to 10 kHz and a lower frequency limit set to 0.2 Hz. An output of 1 mV/UnitOut was set for all amplifiers. The force transducer has a static sensitivity, from 0 N to 5000 N with compression 4.01 pC/ms^{-2} , weighs 21 g and is made of stainless steel, a rubber tip is attached. The microphones are free-field condenser microphones with a sensitivity of 50 mV/Pa .

5.2 Setup

The dimensions of the anechoic chamber is $10 \text{ m} \times 10 \text{ m} \times 8 \text{ m}$ (800 m^3), the background noise level is approximately 17 dBA, and has the operational frequency

range from 75 Hz to 10 kHz (with a mean reflection coefficient < 0.1 , which is equivalent to a sound absorption $> 99\%$)[20].

An impact hammer with a force transducer was used to excite the gearbox, two accelerometers were attached on the gearbox in each measurement test and two microphones were located around the gearbox.

Four different accelerometer positions were measured with two different hammer hit positions. The accelerometers are marked with red and black tape. The microphones stayed at the same positions during the whole measurements, they are marked with green and pink tape. The whole setup is presented in Figure 5.1.

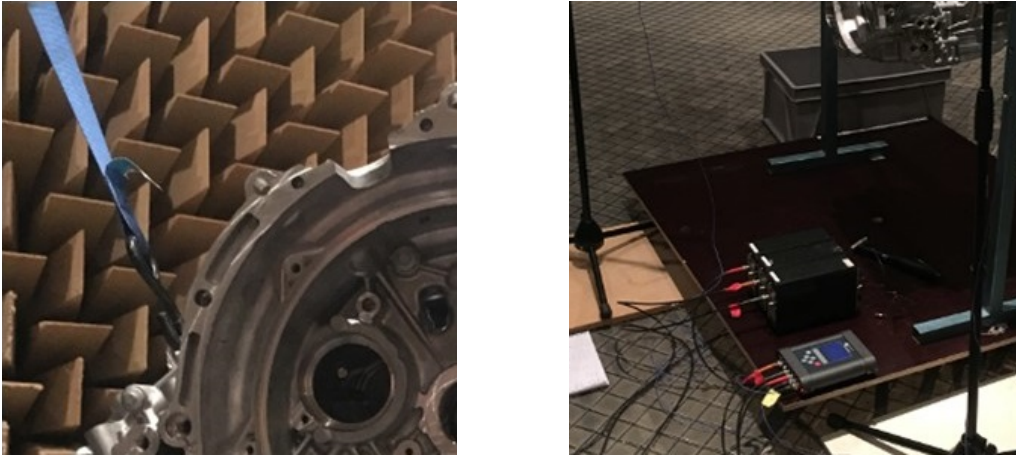


Figure 5.1: Setup of hammer test

A sampling frequency of 12000 Hz was used, this gives the *Nyquist* criterion of:

$$f_{max} = \frac{12000}{2} = 6000 \text{ Hz} , \quad (5.1)$$

which is the frequency range that we are interested in. The *Nyquist* criterion is the sampling theorem to anti-alias the alias affect about high frequency signals showing up as low frequency signals in sampled signals due to lack of time resolution. During the signal analyzing, it is noticed that, 12000 Hz is not a exponentiation, where the base equals to 2, thus, the *Discrete Fourier Transform* was used instead of the *Fast Fourier Transform*. But since the signal sample number was low, the time to calculate was still fast.

5.3 Measurement Positions

Most of the simulation was done before doing the measurements. In the simulations there were some "weak" points where the displacements were high and those same points were measured in test and were compared later in the validation chapter of the thesis. A reference point is used for measuring accelerations inside a testing car, this point is one of the possible vibration transfer path, which was also included as

position 4, shown in Figure 5.6. Excitation of the structure were done in the same way as the modal simulation. One on the casing (HIT Case) and one on the output shaft (HIT Output) position, the positions is presented in Figure 5.2.

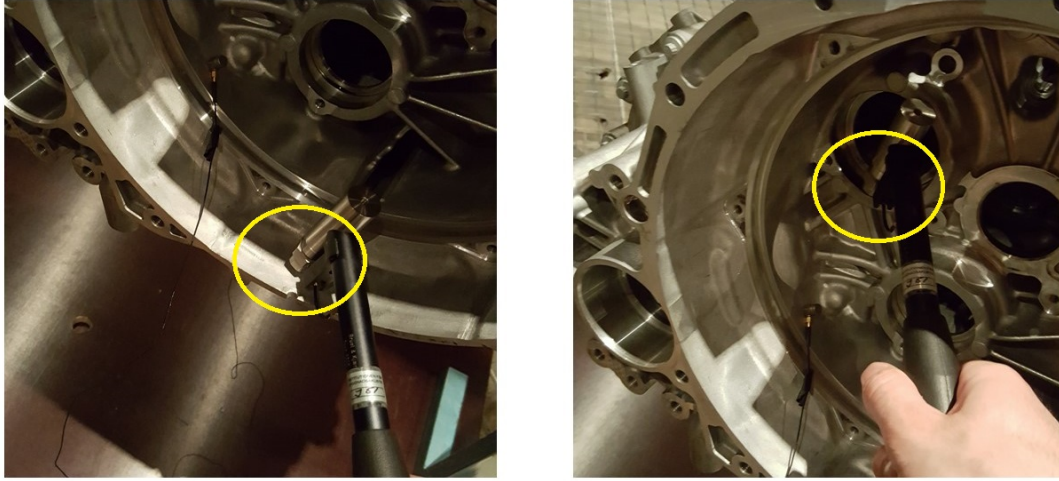


Figure 5.2: Hammer Excitation Positions (HIT Case left side, HIT Output right side)

The accelerometers (two in one group) were placed in four different positions with vax. Locations of the accelerometers are shown on the figures below from Figure 5.3 to Figure 5.6.

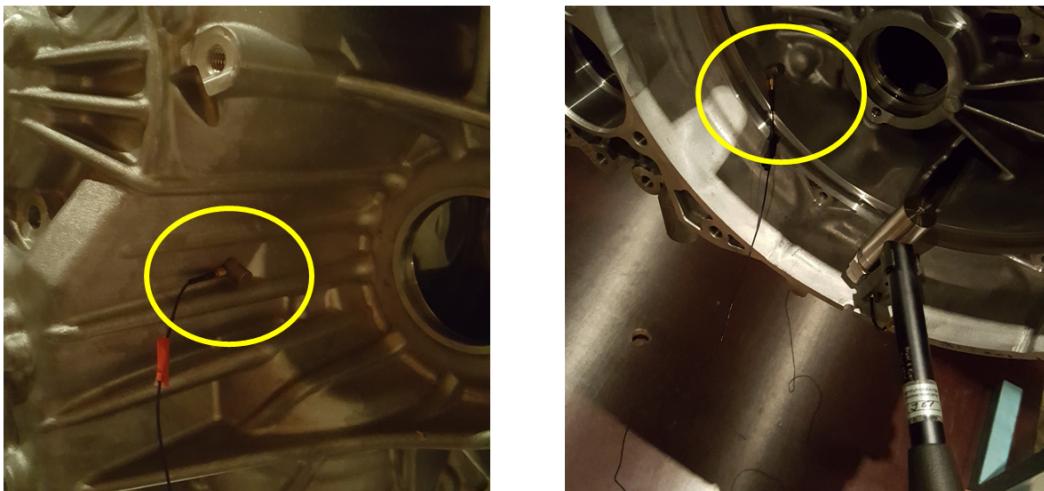


Figure 5.3: Accelerometers position 1

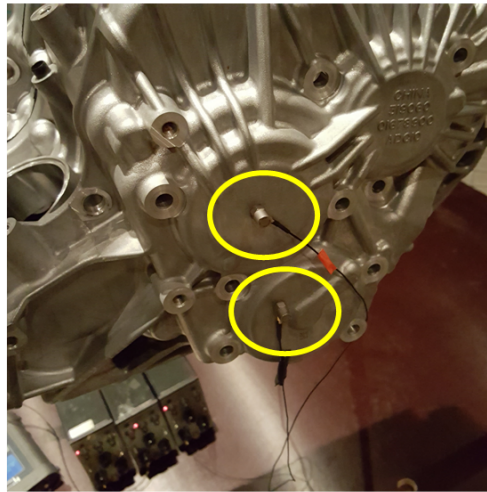


Figure 5.4: Accelerometers position 2

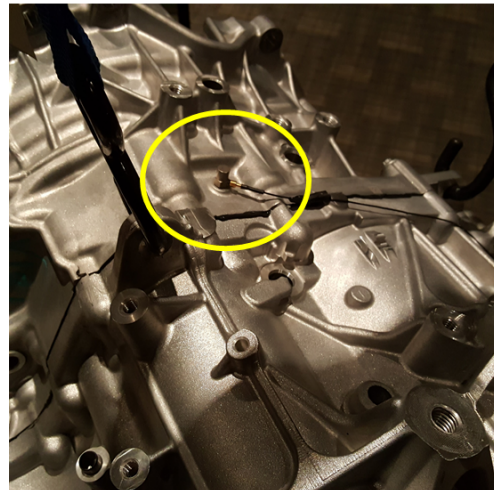
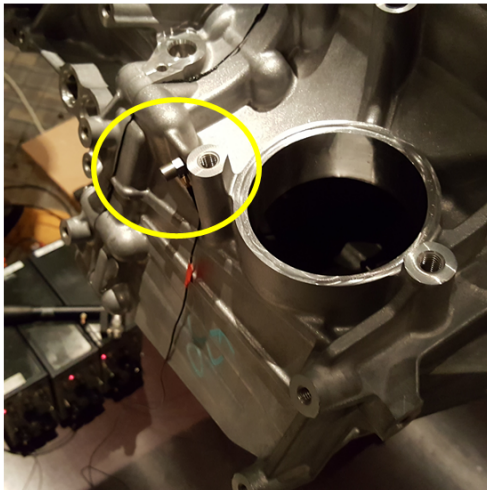


Figure 5.5: Accelerometers position 3

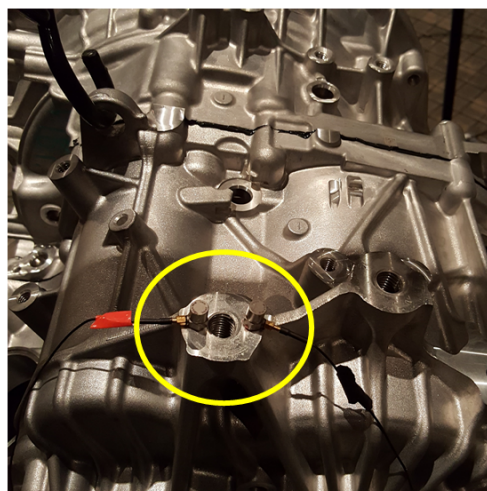


Figure 5.6: Accelerometers position 4

To calculate the transfer function as accurately as possible, at least three hits needs to be recorded for each position, and a total of 25 recordings was performed.

5.4 Signal Processing

The frequency response function is to be calculated in this section. The FRF is used to:

- identify the resonant frequencies, damping and mode shapes of a physical structure
- express the frequency domain relationship between an input (x) and output (y) of a linear, time-invariant system.

The input is the force applied by the hammer ($x = \text{Force} = N$) and resulting accelerations recorded by the output of the accelerometers ($y = \text{Acceleration} = m/s^2$). Generally the input force spectrum should be flat with frequency, as it needs to excite all frequencies uniformly. This is mostly achieved with a shaker and this was not the case for the hammer.

The recordings has sometimes more hits in one recording, therefore, when the hammer hit was registered and then some samples behind and in front needed to be extracted. To locate the sample number for which the hit occurred, this small script was implemented for the first hit:

```
hits = find(H<-10,1); /find the sample that shows -10 N force;
hits = hits-s; /Go back s samples to set a start time;
hite = hits+l; /Go forward l samples to set an end time,
```

and a if loop was implemented for more hits than one.

Once all hits for one recording were extracted. It was plotted to see if there were bad measurements inside it. A bad measurement is defined as:

- Overload/Under-load on the input hammer, this occurs if the hammer hit too hard/soft on the structure and the force transducer gets over/under-loaded
- Overload/Under-load on the accelerometers, this is dependent on the hammer hit
- Bad microphone recording, can be sorted out and not looked at, a bad recording is when someone talks during measurement and this can give a slightly incorrect *Fourier Transform* of the signal.

Figure 5.7 and Figure 5.8 indicate two recordings on the HITCase, the good measurement has a hammer hit that is lower than the limit of -41.51N while the bad measurement has higher hits, as the applied force is unknown, the transfer function cannot be calculated accurately. The "triangle" is the response from the structure caused by the hammer hit, the rest is noise and is cut-off.

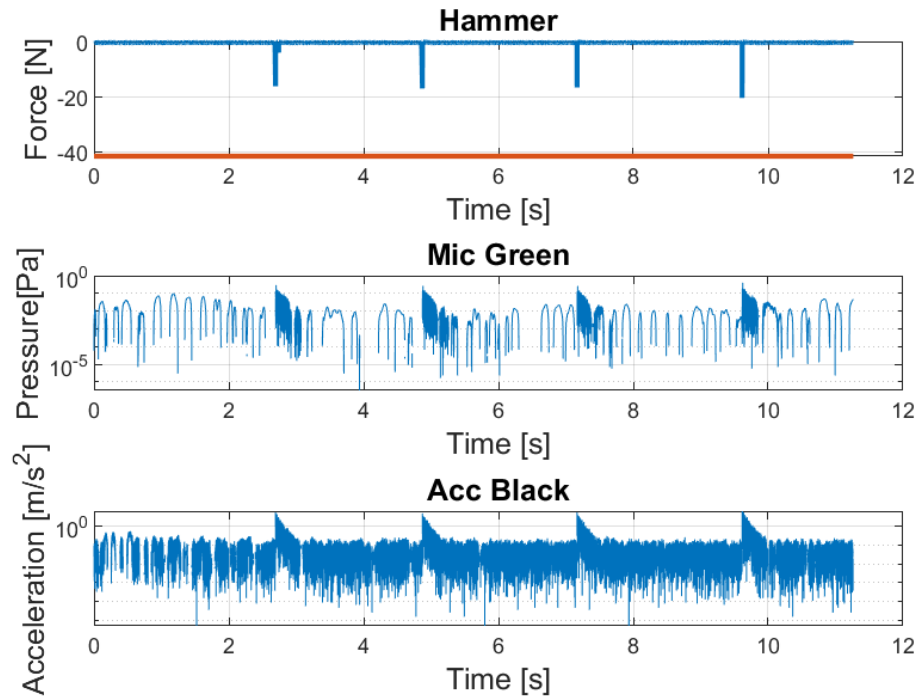


Figure 5.7: Example of Good Measurements

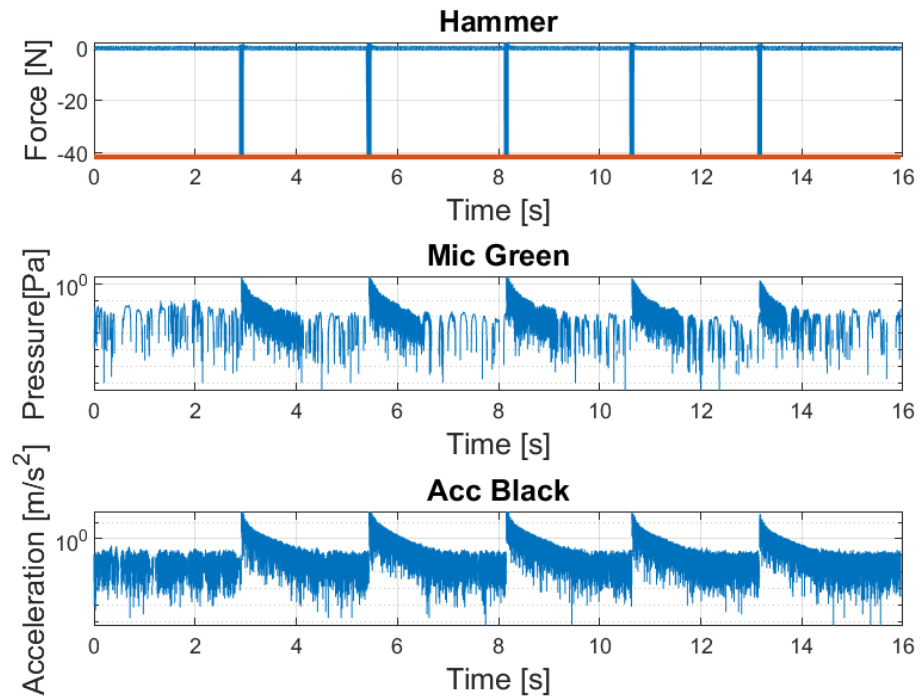


Figure 5.8: Example of Bad Measurements

One of the data extracted is shown below, in the Figure 5.9, which is the cleaned Position 1 Case hit, it has four hits with four blocks.

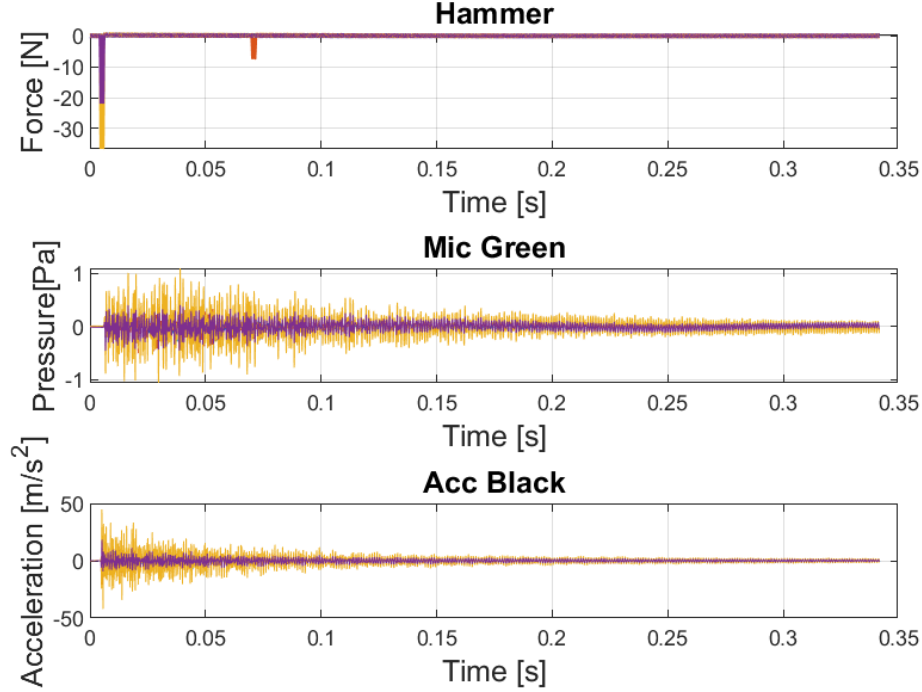


Figure 5.9: 4 Hits From POS1CASE

Once the recordings were cleaned and all the bad measurements were removed, it was time to analyze it with the signal analyzer[21].

No windowing was used as this is a transient signal that decreases sufficiently within the period time and that is the general approach for this kind of signal[21].

The *Fourier Transform* is used to take time signals and transform it into the frequency domain:

$$X(k) = \sum_{n=1}^N x(n)e^{-j2\pi \frac{(k-1)(n-1)}{N}} . \quad (5.2)$$

In Matlab the command is:

`X=fft(x);` .

Squaring the absolute value of the resulting transformed X gives us the double sided auto spectra. It is used when presenting data as it is a measure of the power/energy in the signal. If the conjugate of X is multiplied with Y, this gives us the double sided cross spectra, these are shown in formula:

$$\begin{aligned} S_{xx}(f_n) &= \overline{X(f_n)} \cdot X(f_n) = |X|^2 , \\ S_{xy}(f_n) &= \overline{X(f_n)} \cdot Y(f_n) . \end{aligned} \quad (5.3)$$

This was written as the following in matlab:

```
Sxx = abs(x_fft).^2;
Sxy = conj(x_fft).*y_fft; .
```

Transforming a hit in one block would result in showing properties the signal has over that instance. But dividing the signal and also averaging the spectra over every block will result in finding out the underlying properties the signal have. Each block is one hit with the hammer. Averaging of the double sided spectra is implemented as:

```
if in==1
ASxx = Sxx
else
ASxx = ASxx-(ASxx-Sxx)/in
end; ,
```

where `in` is the latest block, and the number of block `NB = 1,2,3...`

To get a good transfer function, a minimum of three blocks (hits) are required.

Single sided spectrum and the amplitude correction is implemented as:

```
AGxx(1) = ASxx(1);
AGxx(2:(N/2-1)) = 2*ASxx(2:(N/2-1));
AGxx(N/2) = ASxx(N/2); .
```

The relation between the two signals is the *Frequency Response Function* (FRF) or *Transfer Function*. This is implemented by dividing the single sided cross spectrum with the single sided auto spectrum. The function A is the relation between these signals, what happens to the input signal is that after it has passed through the system and then it is output-ed (LTI) as:

$$\begin{aligned} Y(f_n) &= A(f_n)X(f_n) , \\ A(f_n) &= \frac{Y(f_n)}{X(f_n)} . \end{aligned} \tag{5.4}$$

Dividing the cross-spectrum with the auto-spectrum gives us the H1 estimated, calculated in Equation 5.5.

$$H_{xy,1}(f_n) = \frac{AG_{xy}}{AG_{xx}} . \tag{5.5}$$

The frequency response function is implemented as:

```
H1 = AGxy./AGxx;
H2 = AGyy./AGxy;
H3 = (H1+H2)/2; .
```

The H1 is the most commonly used, which assumes that there is no noise on the input and consequently that all the X measurements are accurate. All noise is assumed

to be on the output Y . The H2 is opposite, where the output is seen as accurate, it is assumed that the input contains all noise. The H3 estimator provides the best overall estimate of the frequency function. It approximates to the H2 estimator at the resonances and the H1 estimator at the anti-resonances.

In this case the inertance is of importance, since we are working with vibrations where the input is force (N) and the output is acceleration (m/s^2), inertance is:

$$Inertance = \frac{Acceleration}{Force} = \frac{m}{Ns^2} . \quad (5.6)$$

Presenting the mobility is more common as it gives a rather flat spectrum, the mobility is defined as:

$$Mobility = \frac{Velocity}{Force} = \frac{m}{Ns} . \quad (5.7)$$

Velocity is acceleration integrated with time:

$$v(t) = \int_{-\infty}^t a(t)dt . \quad (5.8)$$

In the definition of FFT, shown in Equation 5.2, the integration corresponds to a division with $j2\pi f$. The value when the frequency is $f = 0$ is discarded, since it cannot divide by 0. The script for mobility is shown below:

```
Ymob2=H2(2:end)./(1i*2*pi*freqnb(2:end)); .
```

For the microphones the FRF is slightly different, where here there is pressure instead of acceleration:

$$FRFMIC = \frac{Pressure}{Force} = \frac{Pa}{N} . \quad (5.9)$$

The microphone data is attached to Appendix B.

5.5 Results

This section will focus on Position 1 Case Hit, shown in Figure 5.3, the right picture that is the black accelerometer against the hammer. First look at the single sided spectra, it can be seen that the Force that is the hammer has a downward slope that bounces at 2.4 kHz and then at 3.2 kHz. While in the higher frequencies it is mostly noise, this indicates that insufficient energy is input-ed across the frequency range of interest. We learned that this was the result of using a rubber-tip on the hammer. The head should have been switched to a steal-tip instead, this would have resulted in the first bounce being in the higher frequencies, instead the rubber damped the hit.

Up to 800 Hz the spectra are almost flat, this is the result of the gearbox hanging freely, the energy just makes the gearbox swing and not vibrate.

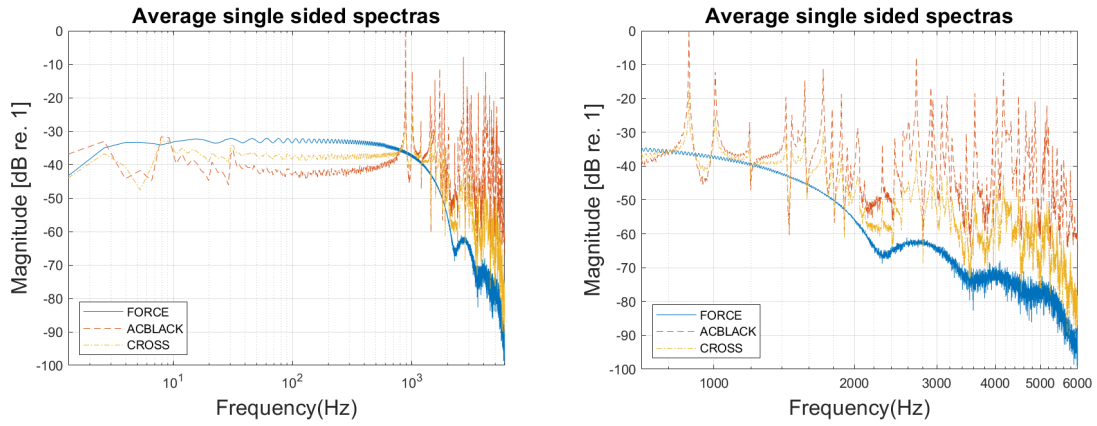


Figure 5.10: Full frequency and cut-off from 500Hz

When the amplitude of a FRF (H estimates) is very high, for example at a resonant frequency, the coherence will have a value close to 1. At an anti-resonance, where the amplitude is low, the coherence will have a value closer to 0. This is because the signals are so low, that their repeatability is made inconsistent by the noise floor of the instrumentation, and this is acceptable. When the coherence is closer to 0 than 1 at a resonant frequency, or across the entire frequency range, then we have a problem with the measurement equipment. Comparing the FRF and the coherence resonances and anti-resonances, there is clear indication that it is a good measurement, the only problem found is that in the higher frequencies, we did not get enough energy from the input, from 3 kHz and upwards. Another factor that affects the coherence is that the hammer operator might strike the structure at different angles between impacts and this results in having inconsistent excitation.

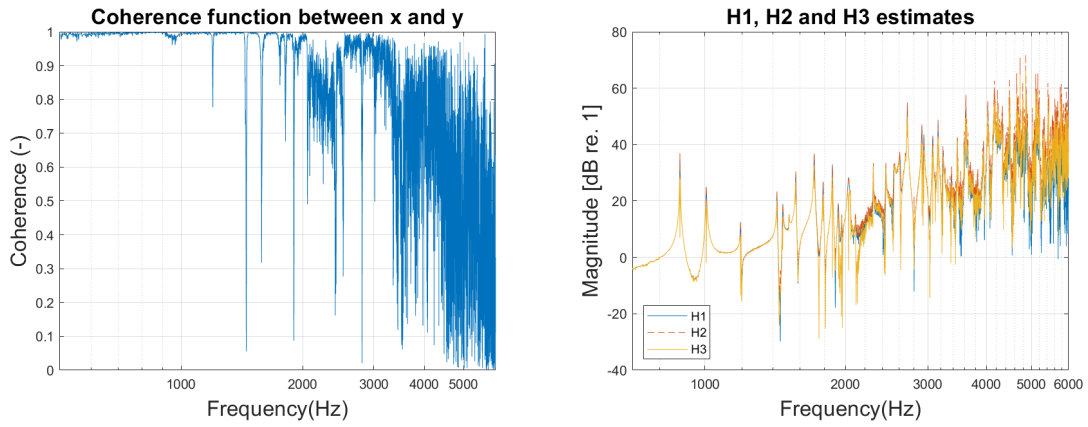


Figure 5.11: Coherence and FRF estimates

More accurate values are given in the H2 estimates thus the Y_{mob2} needs to be studied further. This means that most noise is in the input signal with the hammer. The mobility shows very clear resonance frequencies and anti-resonance frequencies up to 3.4 kHz.

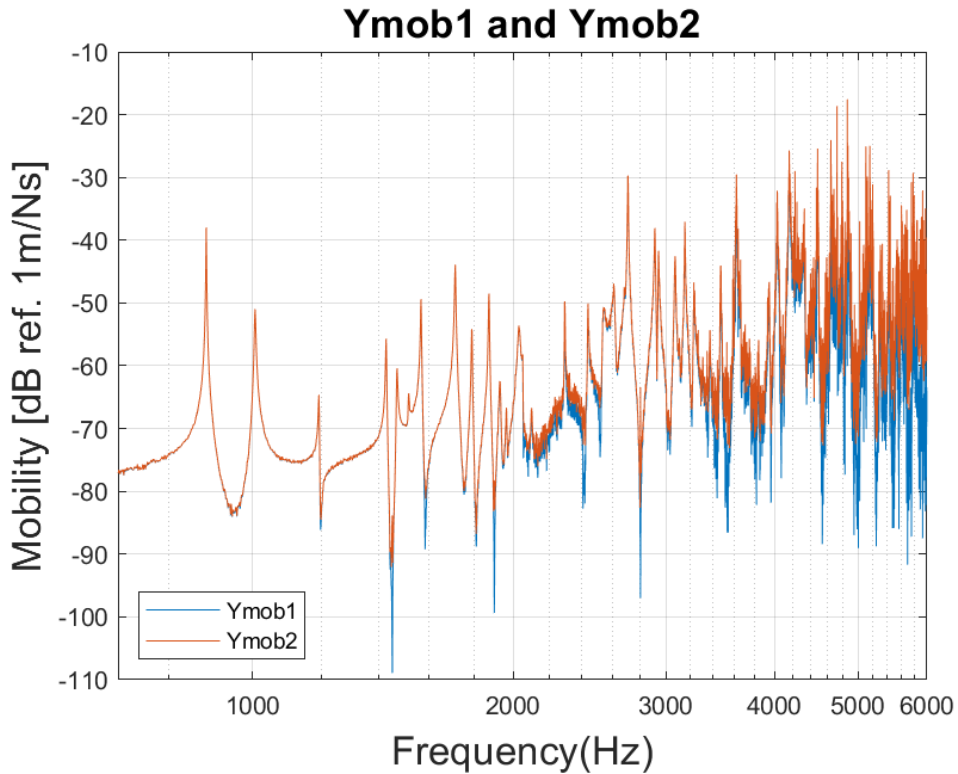


Figure 5.12: Mobility of H1 (Y_{mob1}) and H2 (Y_{mob2})

The FRF is a complex function that contains the amplitude and phase. The amplitude is the ratio of the input force, 1 m/Ns . The phase indicates whether the response moves in and out of phase with the input. The real part of the FRF will equal to zero at natural or resonant frequencies and the imaginary part will have

peaks above or below zero at resonant frequencies. The imaginary part can be plotted to show the mode shapes of the structure, but for a complex structure as this gearbox, many more points has to be measured to get accurate mode shapes.

$$\begin{aligned} Amplitude &= \sqrt{Imag^2 + Real^2} , \\ Phase &= \tan^{-1} \left(\frac{Imag}{Real} \right) . \end{aligned} \quad (5.10)$$

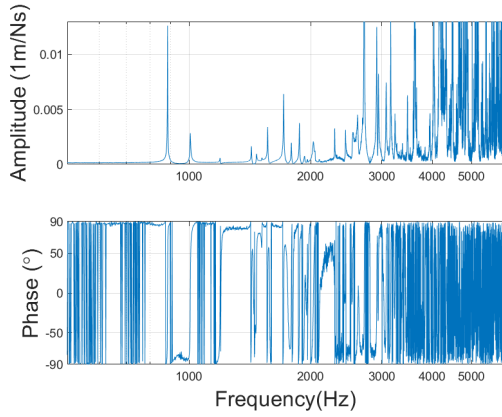


Figure 5.13: Amplitude and Phase

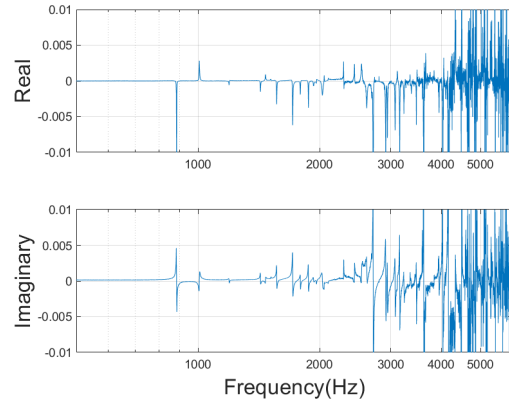


Figure 5.14: Real and Imaginary

When we look at the final mobility plots for the Case Hit, we can see clear resonances and anti-resonances. The first resonance frequency is at 885 Hz which is also the one with the highest amplitude, and the second resonance occurs at 1007 Hz. The third peak is an anti-resonance for Position 1 and a resonance for the other Positions at 1200 Hz.

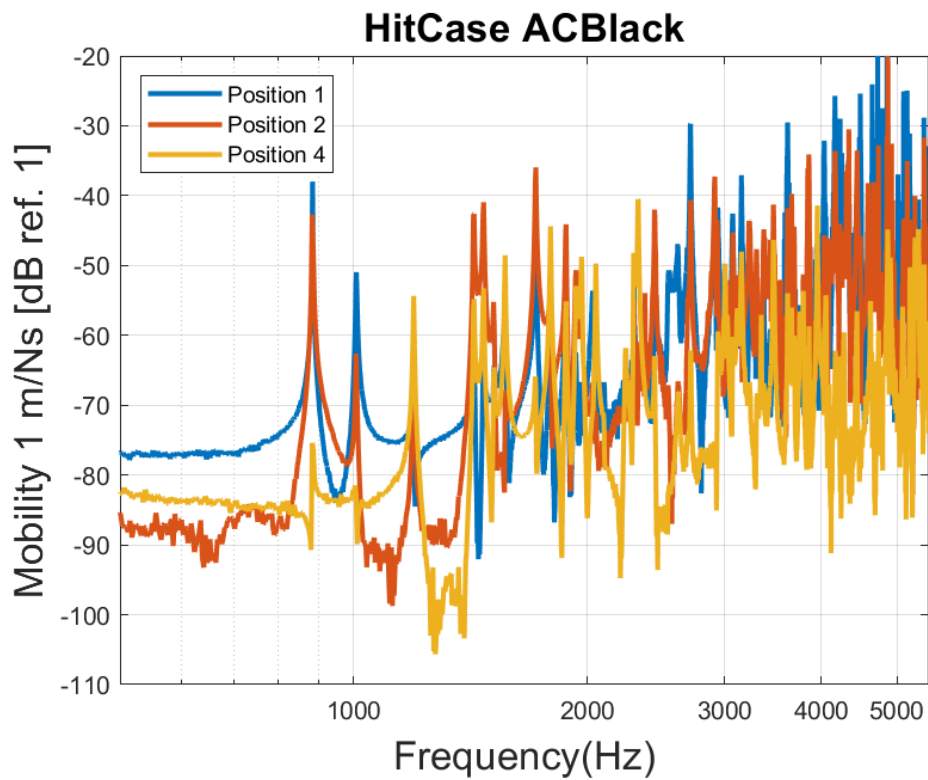


Figure 5.15: "HITCASE" positions 1, 2 and 4

Hitting the Output gives slightly different results. Now a quite noisy resonance occurs at the first peak at 772 Hz but only for Position 1. Here the resonance at 1200 Hz is much higher while the first three resonance is lower. Different hits excite the resonance frequencies differently, thus, to get a good understanding of clonk noise, a similar excitation needs to be tested.

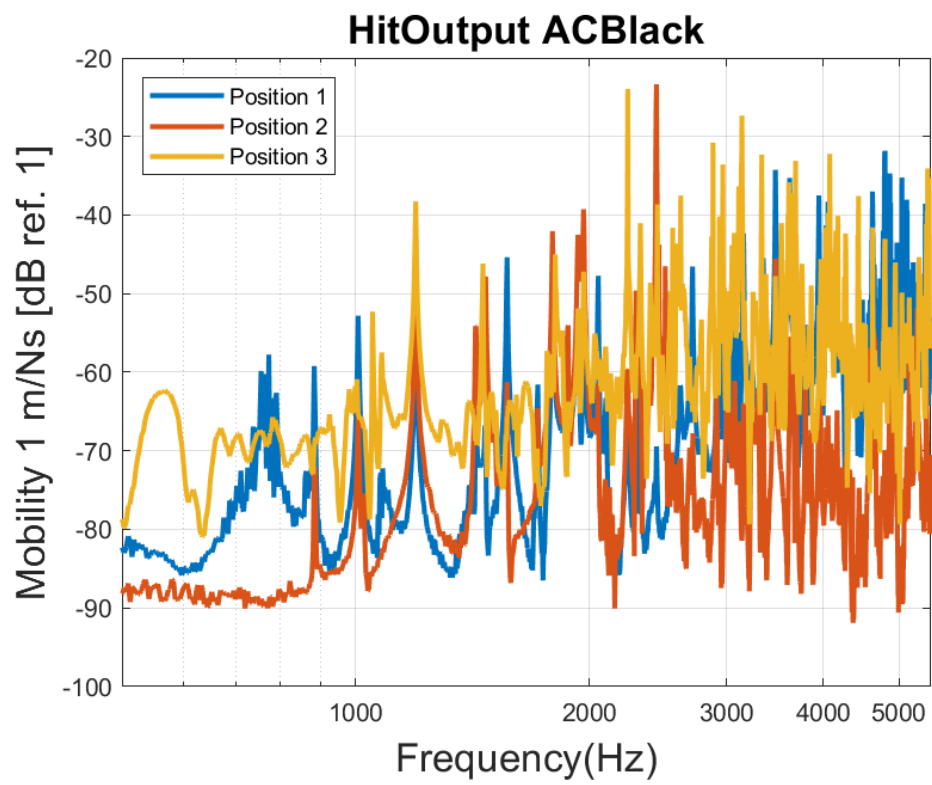


Figure 5.16: "HITOUTPUT" positions, 1, 2 and 3

6

Validation

After the measurement and the signal processing was completed, the measurement results were correlated with the simulation results. To give a more precise comparison, the damping factor of the measurements are imported to the simulation. The damping factors are calculated by using the half-power bandwidth method, the equation is shown below:

$$\eta = \frac{\Delta f}{f_n} = \frac{f_2 - f_1}{f_n}, \quad (6.1)$$

where f_2 and f_1 is the upper and lower limit of the bandwidth 3 dB below the peak of the transfer function magnitude, respectively, f_n is the resonance frequency of the current peak. The half-power bandwidth is illustrated in Figure 6.1.

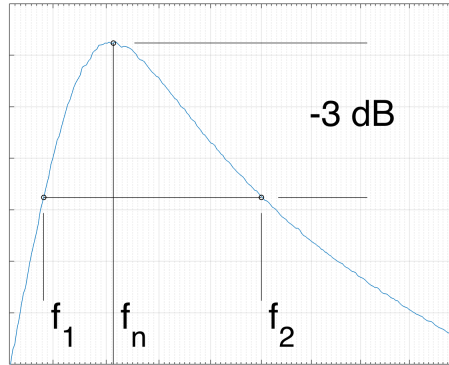


Figure 6.1: Illustration of the half-power bandwidth method

The calculated damping factor in frequency spectrum is given in Table 6.1, which is an average of the transfer function H2. The damping factor reaches very low values at high frequencies, as the damping factor is independent with the frequencies, this can be the result that at higher frequencies, only local modes are excited and the other parts are not so important, which results in lower amplitude of the damping factor.

Frequency	η
0	0.01
885	0.01
1007	0.00006
1193	0.001
1427	0.003
1714	0.0008
2713	0.0008
3617	0.00088
4226	0.00012
5019	0.0001
10000	0.0001

Table 6.1: Damping factors

The same positions that have been measured is to be compared with the simulation results.

When we compared the initial values of the simulation results with the measurement data, the area of the force applied is like comparing a hammer surface with a needle. There are two adjustments to simplify this problem, either spread the force over more nodes or lower the force applied. We proceeded to lower the force to 0.01 N , since:

$$\begin{aligned}
 Hammerarea &\approx 1cm^2 = 0.0001m^2, \\
 P &= \frac{F}{A} = \frac{1}{0.0001} = 10000N/m^2, \\
 F_{sim} &= P \cdot A_{node} = 10000N/m^2 \cdot 0.000001m^2 = 0.01N.
 \end{aligned} \tag{6.2}$$

A change in the damping factor results in the peaks being greater, also there is a shift of the resonances. To correct the shift a change in the Young's modulus needs to be applied for the simulation i.e lower frequencies are needed to give the same mobility. After testing several values, the best results were reached by lowering the Young's modulus to 54 GPa from 71 GPa .

The results is presented in two sections, vibration and acoustics.

6.1 Vibration

The accelerometers that were used to do the measurements is only valid in one direction, the normal of the surface. Whereas the simulation is able to calculate all three axis, in X, Y and Z direction, thus, we need to only extract the normal direction, so that a comparison to the measurement can be accomplished. The normal direction defined for all four positions are shown in Table 6.2.

NODE	Direction
POS1	45° X and Z
POS2	Y
POS3	Z
POS4	Z

Table 6.2: Normal direction relative to the simulation

But this assumes that we hit the structure perfectly in Z-direction. Which is not the case, thus when we compare these measurements points with the simulations, it is not accurate and should only be used as a rough validation.

HITCASE position 1, shown in Figure 6.2, results show that the two first resonances that occurs in the measurement is correlated with the measurement data. The resonances match at 880 Hz and 1000 Hz. Since POS1 uses both x and z direction it validates better with measurements.

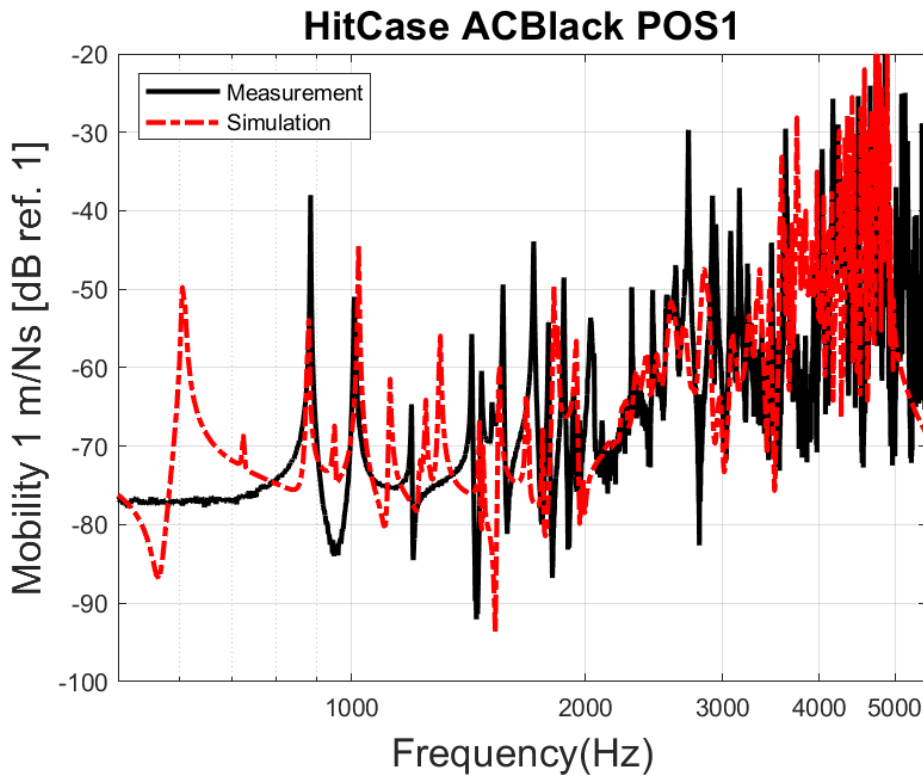


Figure 6.2: Validation of ACCBlack for Case hit, POS1

While the other positions is not as closely validated, this is seen for POS3 and POS4 as shown in Figure 6.3 and Figure 6.4. This is expected as we do not hit the structure perfectly in the z direction, while the simulation does, this might be the reason we get such different results in the other positions. This could also be the results of the measurements being not good.

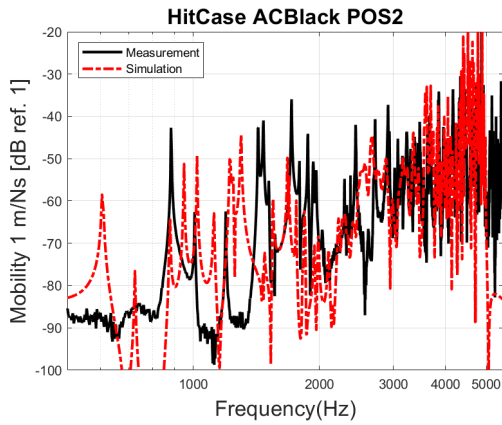


Figure 6.3: ACCBlack, Case, POS2

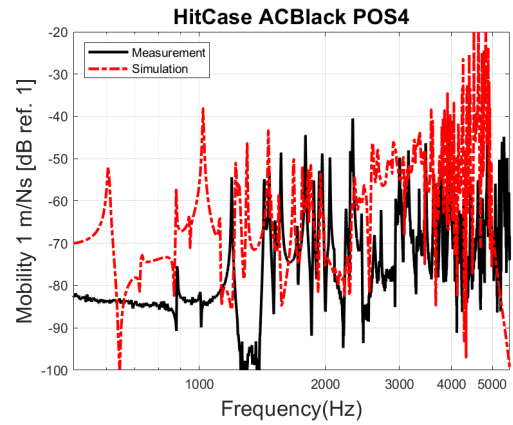


Figure 6.4: ACCBlack, Case, POS4

In HITOUTPUT POS 1, shown in Figure 6.5, We have another resonance that shows in the measurement and simulation at 750 Hz, while the measurement shows a noisy resonance, the simulation results in a clear peak. We have the same matching at 880 Hz and 1000 Hz, except there is another resonance for the simulation at 950 Hz.

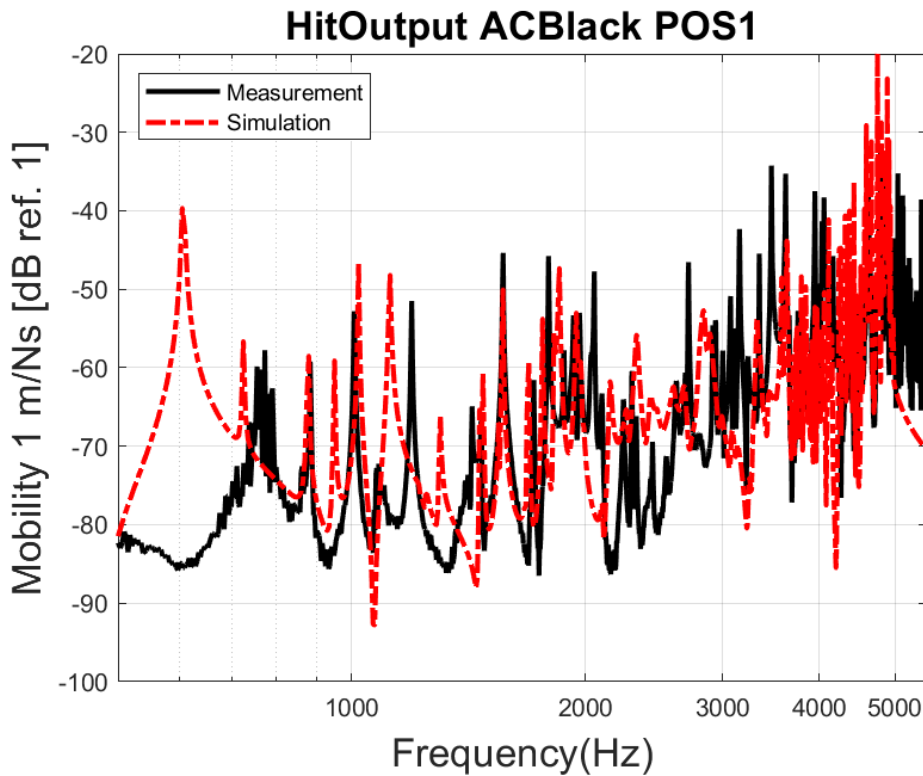


Figure 6.5: Validation of ACCBlack for Output hit, POS1

In HITOUTPUT POS2 and POS3, shown in Figure 6.6 and Figure 6.7, the validation shows matching anti-resonances at 1000 Hz.

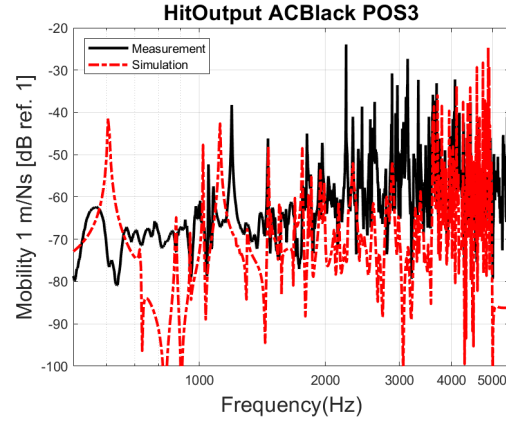
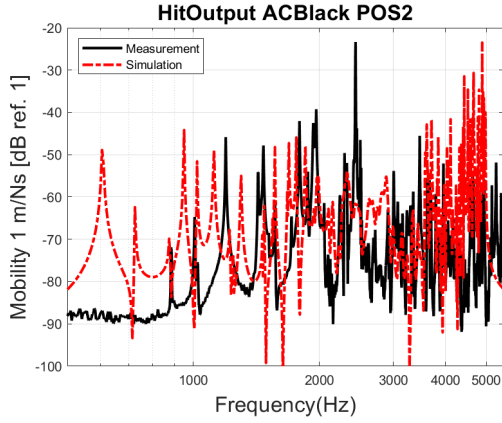


Figure 6.6: ACCBlack, Output, POS2 **Figure 6.7:** ACCBlack, Output, POS3

6.2 Acoustics

The ERP results can be compared with the microphone measurements by the basic formula shown below with some assumptions made,

$$L_p = L_w + 10 \log \left(\frac{DF}{4\pi r^2} + \frac{4}{A'} \right), \quad (6.3)$$

where L_p is sound power level, L_w is ERP, DF is the directivity factor, r is the distance between surface and microphone, and A' is the area of far field i.e. reflections area of the room.

As the measurement is done in the anechoic chamber, this means $A' \approx \infty$, $\frac{4}{A'} \approx 0$ and $DF = 1$. The microphones are placed less than $1m$ from the gearbox, thus, the simulation results, Equivalent Radiated Power (L_w), is calculated approximately:

$$L_p - L_w = 10 \log \left(\frac{1}{4\pi \cdot 1^2} \right) \approx -11 \text{ dB}, \quad (6.4)$$

This means that the ERP values needs to be reduced by 11 dB so that a comparison with the microphone measurements can be done. The ERP is calculated across the entire gearbox, while the microphones is placed on two sides, this is not an accurate comparison but it is still useful to get an early understanding of the sound radiation.

The microphone standing in the front of the gearbox is marked with green tape, it is validated with the ERP results, shown in Figure 6.8 and Figure 6.9. The first resonance that showed up in all the simulation results at 600 Hz is also present when we were recording the position 4 hits. The same resonances seen at 880 Hz and 1000 Hz is also present in the microphones and ERP results, and they are matching.

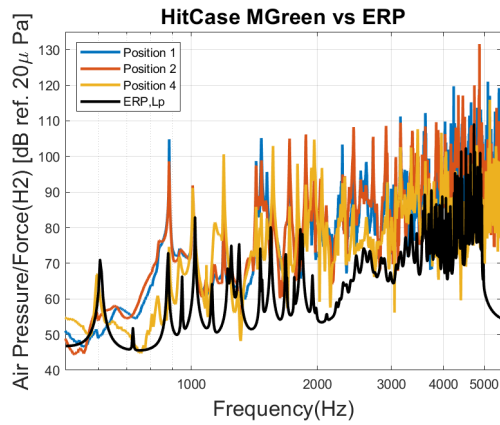


Figure 6.8: Mic Green, Case

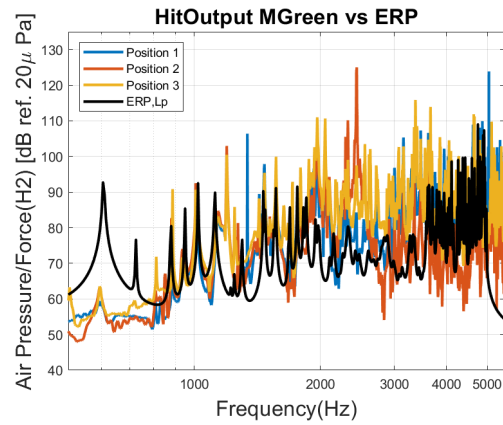


Figure 6.9: Mic Green, Output

Pink microphone is the one standing in the right side of the gearbox. The first resonance at 600 Hz is present in the Pink microphone for all measurements positions. Since the Pink microphone is on the right side of the structure, this means that this first resonance is located on the right side of the structure, further studies in the form of placing accelerometers on the right side so that the location for this resonance can be found and countermeasures applied.

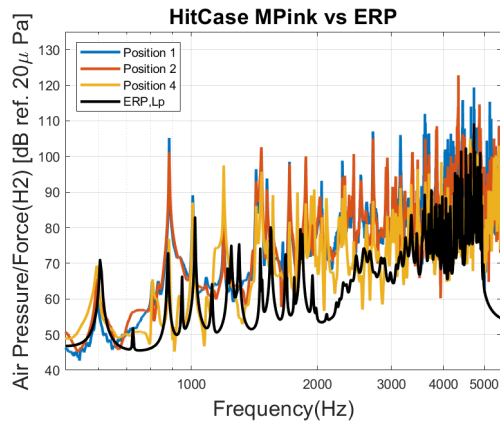


Figure 6.10: Mic Pink, Case

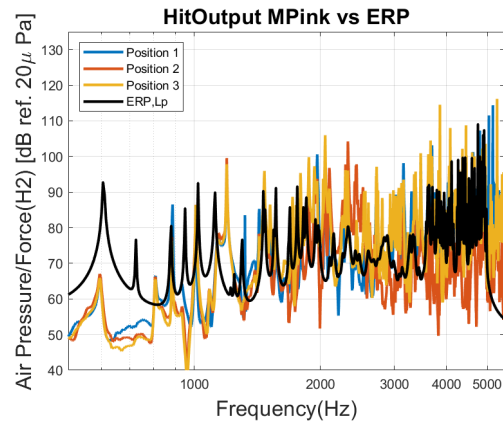


Figure 6.11: Mic Pink, Output

All figures is also presented in 1/3rd Octave Bands in Appendix B.1

7

Conclusion

The simulation result shows good consistency in the first two resonances but differ in the higher frequencies while still having the same characteristics. This is logical since the measurement data is not reliable at higher frequencies than 3 kHz thus a good comparison is not viable.

The overloaded hammer hits in the measurement are excluded. For a more accurate measurement, the hammer hits should be softer to calculate more accurate transfer functions. Also, the tip of the hammer should be changed to a more stiffer one(steel), to excite higher frequencies. More hits per transfer function should be considered.

The ERP Skin should be split into smaller parts of the structure, to locate the position where it radiates most sound. Once it is found, countermeasures like strengthening that part should be focused on. This will result in smaller displacements and less noise radiation. However, the ERP method is not recommended to use in this case, but Actran simulation can be used to solve the problem in the future work.

The correct force that clonk causes to the gearbox should be simulated with gear models, and imported to this simulation. This will give better excitation of the gearbox so that more accurate calculations of the velocities of the structure can be performed.

Another interesting topic is that some car manufacturers that uses electrical engines, output combustion engine noise through the speaker systems to give the driver the imaginary feeling of driving a combustion engine car and also to mask the transmission noise. This could also be studied further for future clonk solutions.

Bibliography

- [1] Robert Fischer, Ferit Küçükay, Gunter Jürgens, Rolf Najork, Burkhard Pollak, *The Automotive Transmission Book*, Chapter 6, page 260, Springer International Publishing Switzerland (2015).
- [2] Harald Naunheimer, Bernd Bertsche, Joachim Ryborz, Wolfgang Novak, *Automotive Transmissions*, Chapter 6, pages 140 - 240, Springer Berlin Heidelberg, 2 edition (2011).
- [3] Robert Fischer, Ferit Küçükay, Gunter Jürgens, Rolf Najork, Burkhard Pollak, *The Automotive Transmission Book*, Chapter 6, page 255 - 259, Springer International Publishing Switzerland (2015).
- [4] Harald Naunheimer, Bernd Bertsche, Joachim Ryborz, Wolfgang Novak, *Automotive Transmissions*, Chapter 12, pages 449 - 560, Springer Berlin Heidelberg, 2 edition (2011).
- [5] Schumacher T, Reitz A, Biermann JW, *Load Reversal Vibration in Motor Vehicle Powertrains – a Compromise Design between Comfort and Agility*, Haus der Technik, Essen (2001).
- [6] Harald Naunheimer, Bernd Bertsche, Joachim Ryborz, Wolfgang Novak, *Automotive Transmissions*, Chapter 7, pages 237 - 274, Springer Berlin Heidelberg, 2 edition (2011).
- [7] L. Cremer, M. Heckl, B.A.T. Petersson, *Structure-Borne Sound: Structural Vibrations and Sound Radiation at Audio Frequencies*.
- [8] Wolfgang Kropp, *Technical Acoustics I*, Propagation And Radiation Of Structure Borne Sound, Gothenburg (2015).
- [9] Hoefer Carsten, *Technical Acoustics II*, Numerical methods for acoustical problems, <http://www.ta.chalmers.se/content/protected/courses/ta2/LectureNumericalMethods.pdf>, Gothenburg (2015).
- [10] Jean-Christophe Autrique, Frederic Magoules, *Studies of an infinite element method for acoustical radiation*, Journal of Applied Mathematical Modelling, Vol. 30, Elsevier (2006), pp. 641-655.
- [11] David S. Burnett, *A three-dimensional acoustic infinite element based on a prolate spheroidal multipole expansion*, AT&T Bell Laboratories, Whippany, New Jersey 07981 (1994).
- [12] K. Gerdes, *Solution of the 3D Laplace and Helmholtz Equation in Exterior Domains of Arbitrary Shape Using Finite Infinite Elements*, Ph.D. Thesis, University of Texas at Austin, 1996.
- [13] K. Gerdes, *A review of infinite element methods for exterior helmholtz problems*, J. Comput. Acoust. (2000).

- [14] Marinus Leugmair, Hannes Münch, *ADVANCED EQUIVALENT RADIATED POWER (ERP) CALCULATION FOR EARLY VIBROACOUSTIC PRODUCT OPTIMIZATION*, 2017. https://www.researchgate.net/publication/315799640_Advanced_Equivalent_Radiated_Power_ERP_Calculation_for_Early_Vibro-acoustic_Product_Optimization
- [15] Cyprien, *What is frequency response analysis in FEA*, December 8, 2016. <http://feaforall.com/frequency-response-analysis-fea/>
- [16] *Frequency Response - Nastran SOL 111*, Aerospace Engineering, April 1, 2014 <http://www.aerospacengineering.net/?p=2728>
- [17] *Actran 18 User's Guide - Volume 1 Installation, Operations, Theory and Utilities*, Chapter 3, page 269 - 277, Free Field Technologies, a Division of MSC Software Belgium SA, November 28, 2017
- [18] ISO 3744:2010, Acoustics – Determination of sound power levels and sound energy levels of noise sources using sound pressure – Engineering methods for an essentially free field over a reflecting plane.
- [19] Patrik Andersson, *Sound and Vibration Measurements, Lab 5: Basic Vibration Measurements*, http://www.ta.chalmers.se/content/protected/courses/svm/lec_svm_lab5.pdf
- [20] *Applied Acoustics - Facilities*, Division of Applied Acoustics, Chalmers University of Technology, <http://www.ta.chalmers.se/about-us/facilities/>
- [21] Patrik Andersson, *Sound and Vibration Measurements, Lab 4: Signal Analysis Task*, http://www.ta.chalmers.se/content/protected/courses/svm/SVM_Lab4.pdf

A

Appendix - Simulation

Nastran Header

```
NASTRAN BUFFSIZE = 65537
NASTRAN SYSTEM(151)=1
ASSIGN USERFILE = 'ERP.csv' UNIT=50 FORM=FORMATTED STATUS=NEW
```

```
SOL 111
DOMAINSOLVER ACMS
DIAG 8,13
CEND
```

```
$
$
SET 1242
SET 1337
$SET 1243
$
$ Panel definition
$
```

```
$SET 1308
$ERP=1309
$SET 1333
$
TITLE= 2 Hit Locations
SUBTITLE= Two Different Forces: 10N or Measurement Hit
$SPC=1
METHOD= 1
$FREQUENCY= 1
FREQUENCY=1
```

```
SDAMPING= 1
```

```
SUBCASE 1
LABEL=AT 4000-5000Hz
DLOAD= 2
ERP(PRINT,PUNCH, KEY = FREQUENCY , ERPRHO = 1.18E-12 , ERPC = 3.43E+05 , RHOC = 2.E+9 , CSV = 50 )= 1309
VELOCITY(PLOT , PHASE )= ALL
DISPLACEMENT= 1242
RANDOM= 1249
```

```
SUBCASE 2
LABEL=Hammer hit 10N, for 2300Hz, HIT2
DLOAD= 4
ERP(PRINT,PUNCH, KEY = FREQUENCY , ERPRHO = 1.18E-12 , ERPC = 3.43E+05 , RHOC = 2.E+9 , CSV = 50 )= 1309
$VELOCITY(PLOT , PHASE )= ALL
$DISPLACEMENT= 1337
$ACCELERATION= 1337
ACCELERATION(PRINT,PUNCH )= 1333
$RANDOM= 1249
```

```
SUBCASE 3
LABEL=Hammer hit 10N, for 2300Hz, Outputshaft
DLOAD= 6
```

A. Appendix - Simulation

```
ERP(PRINT,PUNCH, KEY = FREQUENCY , ERPRHO = 1.18E-12 , ERPC = 3.43E+05 , RHOCP = 2.E+9 , CSV = 50 )= 1309
$VELOCITY(PLOT , PHASE )= ALL
$DISPLACEMENT= 1337
$ACCELERATION= 1337
ACCELERATION(PRINT,PUNCH )= 1333
$RANDOM= 1249

BEGIN BULK
PARAM, COUPMASS, -1
PARAM, GRDPNT, 0
PARAM, PRGPST, NO
PARAM, TINY, 0.0
PARAM, POST, -1
```

RADACT Procedure

☐ Create an Acoustic Fluid Mesh

☒ Import an Acoustic Fluid Mesh model

Acoustic Fluid Mesh

3D/Solid Element Type

Tetra Rapid

Press the 'Create Acoustic Fluid Mesh' button to proceed.

Create Acoustic Fluid Mesh

Export Acoustic Fluid Mesh

Select a NASTRAN file to export the created Acoustic Fluid Mesh.

Import Acoustic Fluid Mesh

/home/shaohaixiong/Desktop/Link to Base/nastran/7DCTEYTestnasAC3.nas

Select a NASTRAN or ANSA volume mesh model.

Figure A.1: Acoustic Fluid Mesh Pre-Processing

Define PID

32248

Press F1 key, to select the Fluid Mesh Property from screen or Database Browser.

Define Sound Speed

340.

Enter a value for Sound Speed.

Define Fluid Density

1.225

Enter a value for Fluid Density.

Figure A.2: Acoustic Fluid Mesh Properties

Define PID

32246

Press F1 key, to select the Infinite Area Property from screen or Database Browser.

Define Order

15

Enter a value for Radial Interpolation Order.

Define Coordinate System

1

Press F1 key, to select a Coordinate System from screen or Database Browser.

Figure A.3: Acoustic Infinite Domain Definition

Define PID

32245

Press F1 key, to select the BC_MESH Surface Property from screen or Database Browser.

Define Gap Tolerance

0.01

Enter a value for Gap Tolerance (extrude tolerance).

Define Plane Tolerance

0.01

Enter a value for Plane Tolerance (relative tolerance).

Figure A.4: Projection Surface Definition

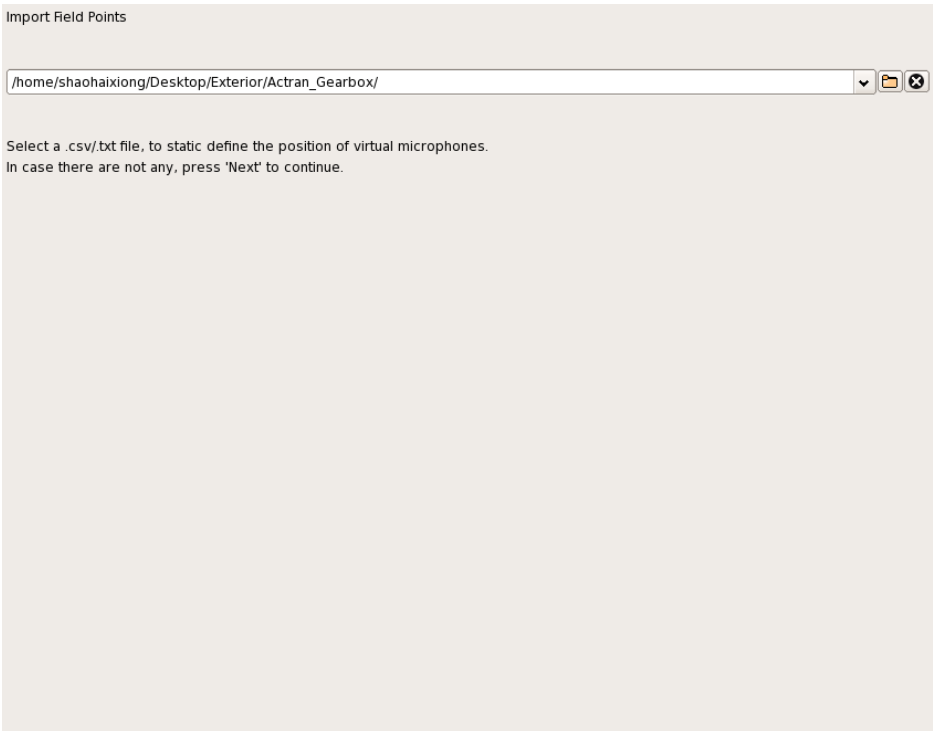


Figure A.5: Acoustic Field Points Definition

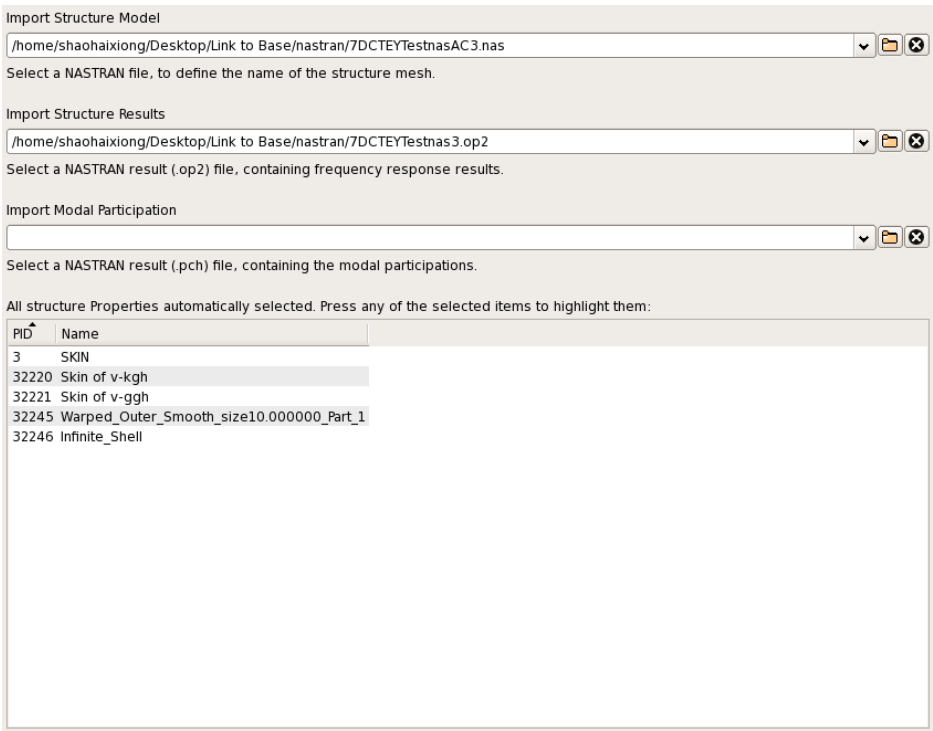


Figure A.6: Structure Import

Frequency List
500 1000 1500 2000 2500 3000 4000 5000
Enter values to define discrete frequencies, separated by space.

Frequency Range
100 100 5000
Enter 3 values to define Freq.Start, Increment and Freq.End accordingly, separated by space.

Define Solver
MUMPS
Select the ACTRAN Solver.

Define Analysis
MODAL_RESP
Select the ACTRAN Analysis.

Contribution Analysis
☐ Panel Contribution
☐ Mode Contribution
In order to allow the post-processing of the Panel/Mode Contribution, check accordingly.

Figure A.7: Analysis Parameters

☒ FIELD /home/shaohaixiong/Desktop/Link to Base/nastran/Field_Points
Define the name of the .plt file output by RADACT.

☒ MAP /home/shaohaixiong/Desktop/Link to Base/nastran/Map_Mesh
Define the name of the .nff results file on the computational mesh output by RADACT.

☐ FIELD_MAP
Define the name of the .nff results file on the field mesh output by RADACT.

Output file (.edat)
/home/shaohaixiong/Desktop/Link to Base/nastran/Output_File
Define the name of the .edat RADACT file.

Figure A.8: Post-Processing Output Files Definition

RADACT Input File

```
BEGIN RADACT

COMMENT_START
  ANSA output file
  for ActranVI v12.0
COMMENT_STOP

BEGIN ACOUSTIC_MODEL_IMPORT

  BEGIN FINITE_DOMAIN
    NASTRAN /home/shaohaixiong/Desktop/Link to Base/nastran/7DCTEYTestnasAC3.nas
    PID 32248
    SOUND_SPEED 340
    FLUID_DENSITY 1.225
  END FINITE_DOMAIN

  BEGIN INFINITE_DOMAIN
    PID 32246
    ORDER 15
    COORDINATE_SYSTEM
    0.00000 0.00000 0.00000
    -40.632534708842 155.263683944598 -24.676365178836
    -41.614838772709 155.449146583437 -24.702486735189
    -40.632192596794 155.404929289514 -23.686390615779
  END INFINITE_DOMAIN

  BEGIN PROJECTION_SURFACE
    PID 32245
    GAP_TOL 0.01
    PLANE_TOL 0.01
  END PROJECTION_SURFACE

END ACOUSTIC_MODEL_IMPORT

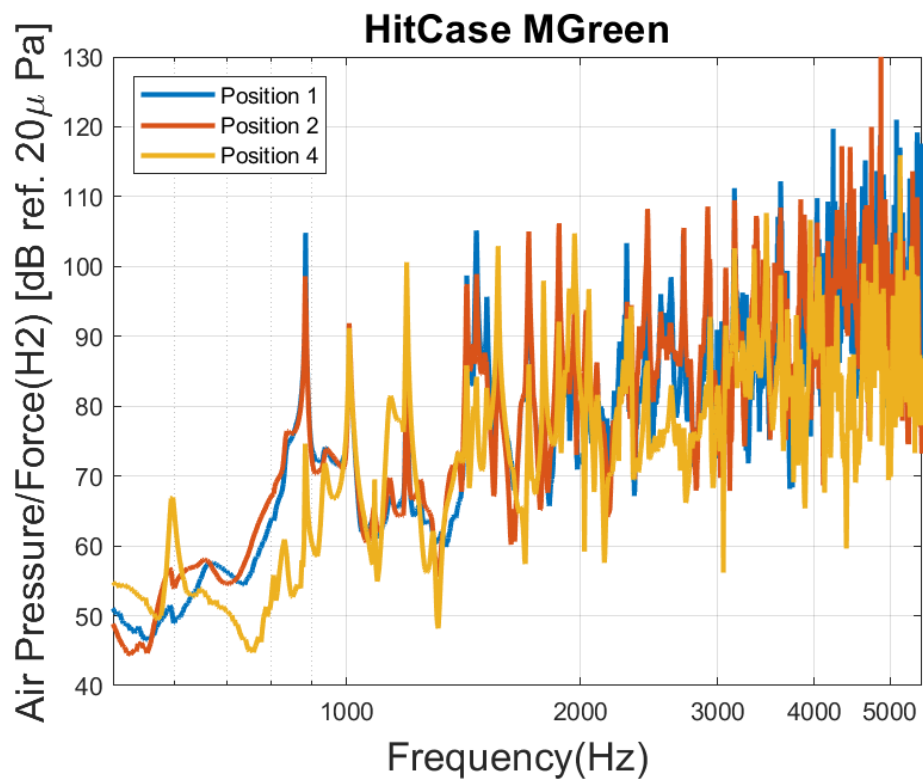
BEGIN STRUCTURE_MODEL_IMPORT
  NASTRAN
  NASTRAN_BC_FILE
  NASTRAN_MODAL_PARTICIPATION
  PID 3 32220 32221 32245 32246
END STRUCTURE_MODEL_IMPORT

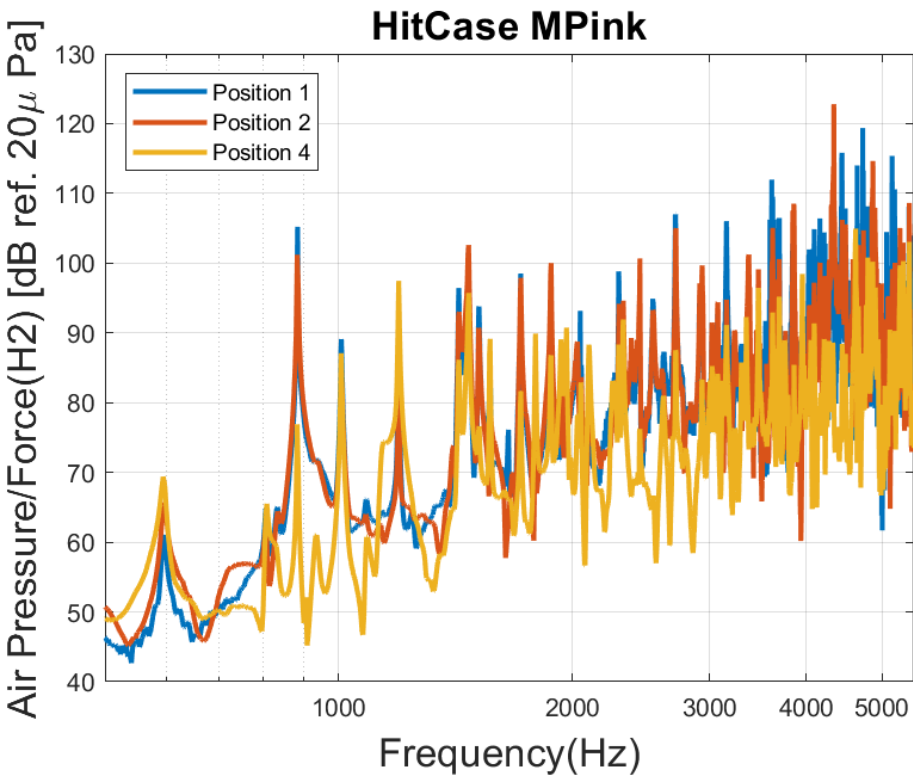
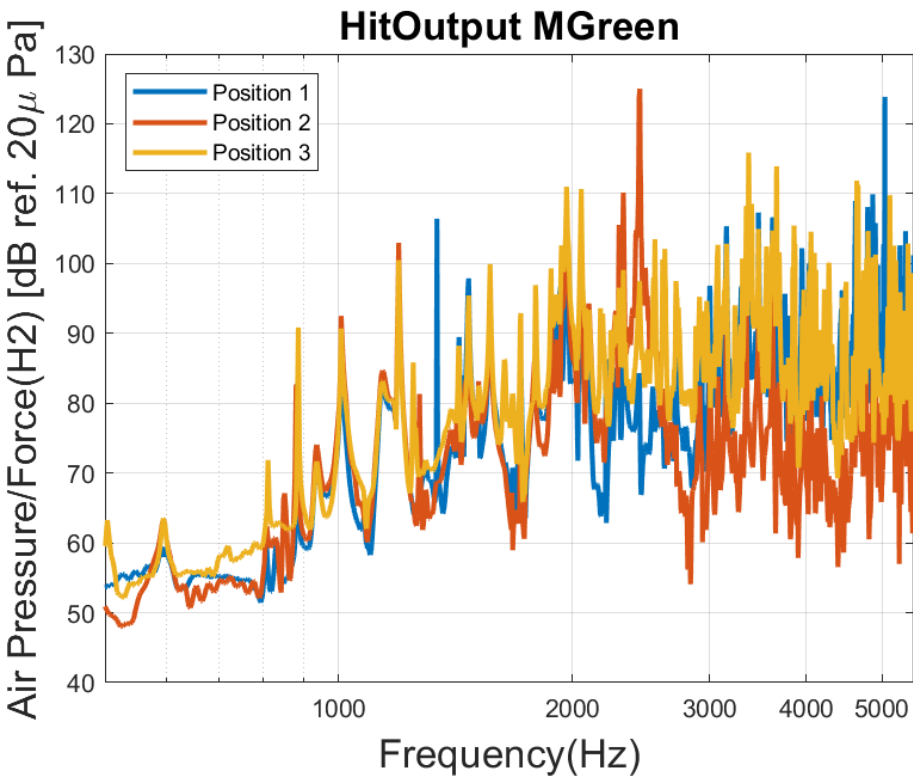
BEGIN RUN_ACTRAN
  FREQUENCY_LIST 500 1000 1500 2000 2500 3000 4000 5000
  FREQUENCY_RANGE 100 10 5000
  SOLVER MODAL_RESP
  MODAL_RESP_ANALYSIS
  PLT_FILE /home/shaohaixiong/Desktop/Link to Base/nastran/Field_Points
  MAP_FILE /home/shaohaixiong/Desktop/Link to Base/nastran/Map_Results
  PANEL_CONTRIBUTION 0
  MODE_CONTRIBUTION 0
END RUN_ACTRAN

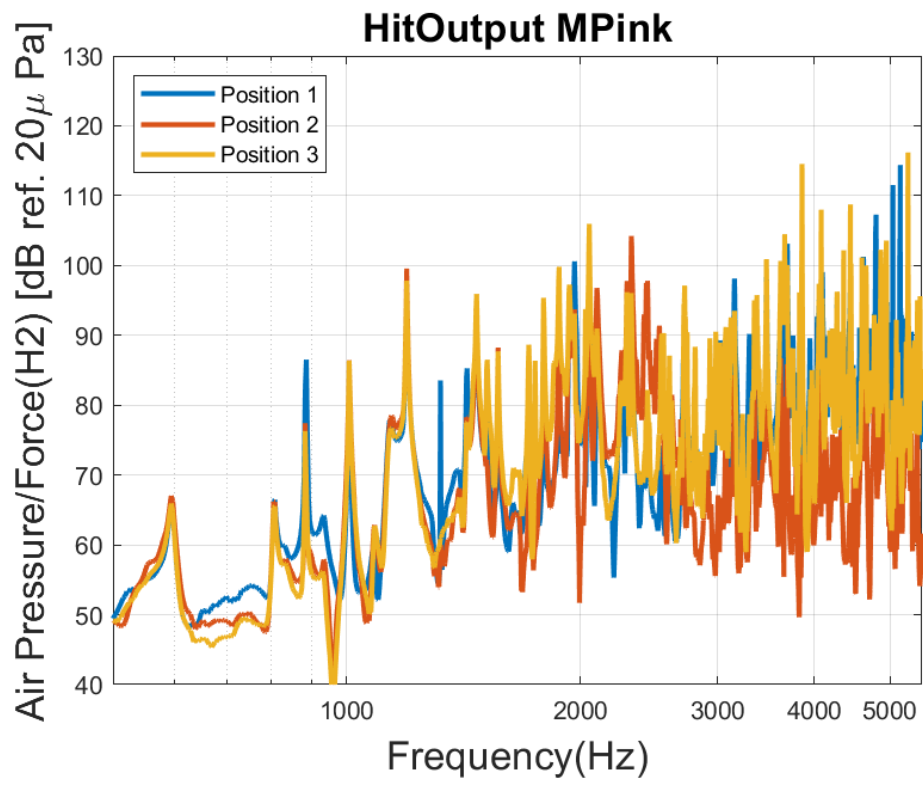
END RADACT
```


B

Appendix - Measurement







B.1 1/3rd Octave band validation

